USGS
science for a changing world

Map and map database of susceptibility to slope failure by sliding and earthflow in the Oakland area, California

By Richard J. Pike, Russell W. Graymer, Sebastian Roberts,
Naomi B. Kalman, and Steven Sobieszczyk

Pamphlet to accompany
Miscellaneous Field Studies Map MF-2385
Version 1.0

2001

U.S. Department of the Interior
U.S. Geological Survey

CONTENTS

ABSTRACT

Map data that predict the varying likelihood of landsliding can help public agencies make informed decisions on land use and zoning. This map, prepared in a geographic information system from a statistical model, estimates the relative likelihood of local slopes to fail by two processes common to an area of diverse geology, terrain, and land use centered on metropolitan Oakland. The model combines the following spatial data: (1) 120 bedrock and surficial geologic-map units, (2) ground slope calculated from a 30-m digital elevation model, (3) an inventory of 6,714 old landslide deposits (not distinguished by age or type of movement and excluding debris flows), and (4) the locations of 1,192 post-1970 landslides that damaged the built environment. The resulting index of likelihood, or susceptibility, plotted as a 1:50,000-scale map, is computed as a continuous variable over a large area (872 km^2) at a comparatively fine (30 m) resolution. This new model complements landslide inventories by estimating susceptibility between existing landslide deposits, and improves upon prior susceptibility maps by quantifying the degree of susceptibility within those deposits.

Susceptibility is defined for each geologic-map unit as the spatial frequency (areal percentage) of terrain occupied by old landslide deposits, adjusted locally by steepness of the topography. Susceptibility of terrain between the old landslide deposits is read directly from a slope histogram for each geologic-map unit, as the percentage (0.00 to 0.90) of 30-m cells in each one-degree slope interval that coincides with the deposits. Susceptibility within landslide deposits (0.00 to 1.33) is this same percentage raised by a multiplier (1.33) derived from the comparative frequency of recent failures within and outside the old deposits. Positive results from two evaluations of the model encourage its extension to the 10-county San Francisco Bay region and elsewhere. A similar map could be prepared for any area where the three basic constituents, a geologic map, a landslide inventory, and a slope map, are available in digital form. Added predictive power of the new susceptibility model may reside in attributes that remain to be explored—among them seismic shaking, distance to nearest road, and terrain elevation, aspect, relief, and curvature.

INTRODUCTION

In the decade since the 1989 Loma Prieta earthquake devastated California's San Francisco Bay region, some 350 natural disasters nationwide have resulted in aid of over $20 billion at the Federal level alone. This assistance has become so costly that mitigation, rather than post-disaster response, is regarded as the way to break the spiraling damage-and-loss cycle (Mileti, 1999; Platt and others, 1999). With Congressional support, the Federal Emergency Management Agency (FEMA) established a pre-disaster mitigation fund to create Project Impact, a partnership between government agencies and the private sector to develop disaster-resistant communities throughout the country (FEMA, 1998). By applying scientific expertise and information, the project seeks to reduce the escalating financial and human losses that result from repeated natural disasters. The city of Oakland was chosen as one of the first seven pilot communities for Project Impact (fig. 1, on map), and adjacent Berkeley followed in 2000. The U.S. Geological Survey (USGS) joined the California Office of Emergency Services (OES), the California Division of Mines and Geology (CDMG), and FEMA in a partnership to increase the resistance of this urban area to rainfall-induced and seismically generated landslides and other types of earthquake hazards.

Slope failure is an expensive problem across the 10-county San Francisco Bay region (Nilsen, Taylor, and Dean, 1976). Damage from landslides alone in the El Niño storms of 1997-98 totaled $160 million in direct costs (about $20 million in Oakland's Alameda County) and several times that amount in indirect costs, such as lost business and wages and increased commuting distances and road-maintenance budgets (Pike and others, 1998; Godt, 1999). Only the epicentral location of the Loma Prieta earthquake in a thinly populated area during a dry season prevented equally serious losses from landsliding. As development of San Francisco Bay area hillsides continues and land values rise accordingly, the economic consequences of slope instability will increase. Moreover, public policy on landslide hazard and risk is so primitive that insurance against most slope failures is not available and the disputes that arise tend to be resolved only through litigation (Stromberg, 1967; Olshansky and Rodgers, 1987; Howell and others, 1999). As the basis for mitigating the landslide hazard, most land-use planning currently relies on either a simple engineering model of slope stability or maps showing ground slope and locations of previous failures.

One obstacle to better public policy is the scarcity of maps showing the likelihood of landsliding over large areas at medium to fine scales (1:50,000 to 1:5,000). Such maps are rare because slope instability—like earthquake and other hazardous natural phenomena (Oreskes, 2000)—is very difficult to predict in space as well as time (Haneberg, 2000). Until recently, maps that delimit the probable extent of flooding or earthquake shaking in the San Francisco Bay region have had few counterparts that delineate the landslide hazard. Only a generalized map of the entire Bay area (Nilsen and Wright, 1979) and one county-scale map (Brabb and others, 1972) have been prepared by USGS. Medium-scale maps by CDMG outline a single hazard zone for earthquake-triggered landslides and carry a regulatory mandate but provide little detail (Wilson and others, 2000). Finer-scale, more detailed CDMG maps indicate areas of potential rainfall- or seismically-induced landsliding and general slope instability but cover small areas (Haydon, 1995; Wills and Majmundar, 2000).

This report describes an experiment to develop a quantitative technique for estimating the relative predisposition, or susceptibility, to certain types of landsliding over large areas. The result is a susceptibility map of the extended Oakland Project Impact area and surrounding hillsides, where slope failure has long posed a hazard (Beaty, 1956; Stromberg, 1967; Nilsen, Taylor and Brabb, 1976; Nilsen and Wright, 1979; Coe and others, 1999). Pike and others (1999a, b) reported earlier results from this experiment, and other USGS work for Project Impact in the East Bay has evaluated methods to predict landslides triggered by earthquakes on the northern Hayward Fault (Miles and Keefer, 2000). The information generated by these studies will assist CDMG, FEMA, OES, and other public agencies in making informed planning and zoning decisions for the San Francisco Bay region.

ACKNOWLEDGMENTS

Reviews by Kevin Schmidt, Earl Brabb, and Scott Graham and remarks by Mark Reid improved drafts of this report.

OAKLAND'S LANDSLIDE HAZARD

Excluding water, the greater Oakland area examined here occupies 872 km^2 on the east side of San Francisco Bay, in the Coast Ranges province of central California (fig. 1). The study area comprises seven 7.5-minute quadrangles: Richmond, Briones Valley, Oakland East and West, Las Trampas Ridge, San Leandro, and Hayward. Climate and the remaining native vegetation are Mediterranean, the highest elevation is 617 m, and slopes at 30-m resolution are as steep as 50° on bedrock outcrops. The northeastern three-fourths of the area is in steep upland ridges and valleys, conspicuously elongated NW-SE and underlain by Mesozoic to upper Tertiary sedimentary rocks (Graymer, 2000). The active Hayward Fault Zone separates the upland (also cut by many small faults) from a flat-lying alluvial plain that borders San Francisco Bay to the southwest. Quaternary deposits veneer the floors of the larger inland valleys and overlie down-dropped upland rocks in the lowland plains (Helley and Graymer, 1997a, b).

The bordering lowland is almost completely urbanized; much of the gentler upland also is settled, mainly in suburbs, which continue to spread into the hills. The study area is primarily residential land (34 percent), forest (28 percent) and rangeland (15 percent); the balance is in diverse urban uses (Association of Bay Area Governments (ABAG), 1996).

Terrain forms and material deposits created by landsliding (Varnes, 1978) are prominent in the hills in and east of Oakland (Radbruch and Weiler, 1963; Radbruch and Case, 1967; Radbruch, 1969). Most of the large landslide deposits that have been mapped in the area (Nilsen, 1975) are presumed to have resulted from earthflow and translational or rotational sliding. Both types of failure involve surficial mantle and bedrock down to depths of a meter to over 50 m, distort the ground surface when they move, and remain as recognizable masses that can persist for thousands of years (Varnes, 1978; Nilsen and Wright, 1979; Keefer and Johnson, 1983; Wentworth and others, 1997). Although slides and earthflows usually move slowly and thus seldom threaten life directly (for a Bay region exception, see Cotton and Cochrane, 1982), they can cause serious property damage. When they move, in response to such changes as increased pore-water pressure, earthquake shaking, added load (graded fill), or removal of downslope support (road cuts), they can offset roads, destroy foundations, and break underground gas pipes and water mains as well as override property. By landslides or slides in this report we mean only these larger failures and their deposits, at least 60 m in the longest dimension and covering a few hectares to several square kilometers.

This report does not address debris flow, a process reflecting a qualitatively different set of geologic, hydrologic, topographic, and meteorological controls and commonly leaving deposits less than 60 m across. This exception has important public-safety implications, because areas that may not be highly prone to sliding and earthflow may be quite susceptible to debris flow, and vice-versa (Haydon, 1995). Commonly termed "mudslides", debris flows are small, shallow mixtures of water, soil, and other debris that mobilize suddenly during locally heavy rains (Ellen, 1988; Dietrich and others, 1993; Wilson and Jayko, 1997) and flow rapidly downslope. Although debris-flow deposits can be extensive and persistent, most failures leave thin, ephemeral fans that do not markedly distort the ground surface (Varnes, 1978). Over time, debris flows may recur in the same location. They are common in the Oakland hills and elsewhere around San Francisco Bay but were not identified explicitly in the set of old landslide deposits analyzed here. Because their recognizable features are quickly obscured by vegetation growth, few debris flows are shown on inventory maps prepared before the San Francisco Bay region's severe 1982 winter (Ellen, 1988).

PRIOR MAPPING OF SUSCEPTIBILITY

Because one clue to the location of future landsliding is the distribution of past movement, maps that show landslide deposits are helpful in predicting the hazard (Liang and Belcher, 1958; Cleveland, 1971; Nilsen, Taylor, and Dean, 1976; Nilsen and Wright, 1979; Cotton and Cochrane, 1982; Wieczorek, 1984; Haydon, 1995; Atkinson and Massari, 1998; Baum and others, 1998; Jennings and Siddle, 1998). Such inventory maps do not necessarily distinguish recent movements, but in any one year some of the mapped slides—or more commonly, portions of them—may become active (Baum and others, 1998; Jayko and others, 1998; Keefer and others, 1998). New landslides in previously unfailed areas also occur, especially where the terrain has been modified by grading (Wentworth and others, 1987). Landslide deposits are well mapped in the San Francisco Bay region. Over 70,000 old (historic but undocumented) and ancient (prehistoric) landslide masses (collectively, hereafter, designated "old") are shown on mostly 1:24,000-scale inventory maps by USGS and CDMG that individually cover small portions of the region (Nilsen and Wright, 1979; Pike, 1997; a few of the approximately 90 maps have scales of 1:12,000 and 1:62,500). These paper maps are being recompiled by USGS as computer databases at 1:24,000 scale and released for each county as 1:62,500-scale plots (Roberts and others, 1998, 1999). Digital coverage is not yet available for the entire Bay area.

A landslide inventory reveals the extent of past movement and the probable locus of some future activity within those slide deposits, but it does not indicate the likelihood of failure for the much larger area between mapped deposits (Brabb, 1995). Blanc and Cleveland (1968) were among the first to devise a spatially complete expression of the landslide hazard for an area in southern California. Based on experience with slope failure, they qualitatively synthesized several of the major controls on slope stability and mapped eight estimated degrees of site susceptibility. Blanc and Cleveland's second innovation was to rank the area's geologic units in four groups of decreasing susceptibility and to assign existing landslide deposits to the highest rank. Van Horn (1972) advanced the concept, incorporating four classes of ground slope and adding terrain other than mapped landslide masses to the highest of four categories of stability. Because they rely on personal expertise, both maps are subjective and difficult to compare; the results are not repeatable nor the procedures of compilation transferable. Cleveland (1971) advocated a more quantitative approach to synthesizing multiple controls on slope failure and listed several candidate variables. Earlier, Jones and others (1961) had statistically correlated landsliding in northeast Washington with three of these site factors: geologic materials, terrain slope, and moisture content.

Efforts by CDMG to map areas of potential slope instability as a guide to land development in the San Francisco Bay region date to Rogers and Armstrong (1971). These relative geologic stability (now relative landslide potential) maps typically show four zones of varied susceptibility that carry no regulatory mandate (Wills and Majmundar, 2000). The zones were interpreted qualitatively by synthesizing field-based studies of rock type, geologic structure, topography, and prior landslide activity as well as potential seismic and rainfall trigger mechanisms. Four such maps cover about half the Oakland Project Impact area (Bishop and others, 1973; Haydon, 1995, Majmundar, 1996a, b). CDMG

currently publishes landslide-zone maps funded by FEMA and OES under the Seismic Hazards Mapping Act (CDMG, 1997) to accompany maps of earthquake shaking (Haydon and others, 2000) and liquefaction (Petersen and others, 2000). Determined in part by adapting methods developed at the USGS, the map by Wilson and others (2000) depicts a single discontinuous zone subject to seismically-induced landsliding for part of the Project Impact area. This map is an official document that requires site mitigation prior to any development, as defined in Public Resources Code Section 2693c (CDMG, 1997).

In the earliest USGS attempt to estimate the landslide hazard continuously over a region, Brabb and others (1972) extended the concept of Blanc and Cleveland (1968) by combining the distribution of old slide deposits, bedrock map-units, and ground slope in a semi-quantitative model of landslide susceptibility (Brabb, 1995). Their test area was the entire San Mateo County, across San Francisco Bay from Oakland. Newman and others (1977) automated this three-parameter model, and Roth (1983) found its results internally consistent. Using the same three variables and the overlay technique pioneered by McHarg (1969), Nilsen and Wright (1979) manually compiled a generalized susceptibility map for the nine-county San Francisco Bay region (less Santa Cruz Co.) at 1:125,000 scale. Whatever their virtues, however, none of the maps described above were compiled from high-quality slope data or distinguished the varied likelihood of future failure within mapped slide deposits.

Geographic information systems (GIS) technology has freed susceptibility modeling from many of its qualitative limitations, and the computer-mapping of landslide susceptibility has spread worldwide (Aniya, 1985; Carrara and others, 1992, 1995; Brunori and others, 1996; Fernández and others, 1996; Soeters and van Westen, 1996; van Westen and others, 1997; Cross, 1998; Dhakal and others, 2000). Although the multi-parameter estimation of susceptibility now is common, its effectiveness is limited in four respects: (1) the resulting maps usually cover small areas (Mora and Vahrson, 1994; Miller, 1995; Massari and Atkinson, 1999); (2) the maps require detailed information, some of it on many parameters, that can not be obtained economically for large areas (Jäger and Wieczorek, 1994; Miller, 1995; Fernández and others, 1996); (3) the maps express susceptibility qualitatively, on an ordinal (high, moderate, low) scale (Aniya, 1985; Hylland and Lowe, 1997; Turrini and Visintainer, 1998); and (4) the maps lack transparency, in that they result from complex computer-analyses wherein input parameters can be difficult to correlate with landslides occurrence and other field observations (Dhakal and others, 2000). The experiment reported here addresses these shortcomings.

SCOPE, ASSUMPTIONS, AND METHOD

In this report we develop a numerical index of landslide susceptibility and map it over an extensive area at a comparatively high resolution. The empirical model estimates relative susceptibility of a site to the two types of deep failure that are most easily recognized from aerial-photograph surveys of large areas of the San Francisco Bay region (Nilsen, 1975): slides and earthflows or a combination of them (Varnes, 1978). Our approach improves the statistical method of Brabb and others (1972), adapts it to 100 percent digital implementation, and calculates susceptibility as a continuous variable. The three essential sets of data—maps showing geologic units, evidence of old and recent landsliding, and terrain slope—exist within USGS in machine-readable form or require little data-gathering beyond digitizing existing maps of landslide deposits. One expression of the new index number, this map, is a possible prototype for quantitative landslide-susceptibility coverage of the 10-county San Francisco Bay region. The statistical approach should be applicable to any area for which the three sets of data are available.

Because no guidelines for mapping the regional likelihood of deep-seated landsliding have been established, all susceptibility models are based on assumptions—in this case six. They follow from our realization that waiting for the data ideally suited to treating the problem as an engineering exercise would delay, perhaps indefinitely, the preparation of this map for Oakland (Cleveland, 1971). Pike and others (1994) reached a similar conclusion in mapping the susceptibility of earthquake-induced soil liquefaction in Monterey County from available USGS data. A more physically based model of landsliding in Oakland would require geotechnical measurements of the material properties of bedrock and surficial mantle as well as better definition of the surficial mantle (Neuland, 1976; Wieczorek, 1984; Ellen and Wentworth, 1995; Miller, 1995). Geotechnical data are unlikely to be acquired in the necessary detail for each geologic unit (many of which are heterogeneous) over the large area required for a regional assessment of susceptibility. Our six assumptions, however uncertain, are as follows:

(1) Failures under climatic conditions that differ from those now prevailing can be manipulated statistically to suggest the locus of future landsliding.

(2) The areal percentage of past failure in a geologic unit reflects the cumulative effects of physical conditions and processes that induce landsliding.

(3) Deposits from past landslides may be used to infer the location of both deposits and source areas of future failures.

(4) Geology, landslide deposits, and ground slope serve collectively as a proxy for engineering data to estimate susceptibility.

(5) The susceptibility of old landslide deposits to later movement exceeds the susceptibility of areas between them.

(6) The higher likelihood of future movement within old deposits can be estimated from an analysis of recent failures.

Our method departs from that pioneered by Brabb and others (1972) in several respects. We subdivide each geologic unit into much finer, one-degree, intervals of ground slope, and calculate susceptibility for each interval. Our topographic data also are more accurate and our unit-cell size is smaller. Like Brabb and others (1972) we treat old landslide deposits differently from the terrain between them, but rather than assigning the maximum susceptibility value to the entire mass (Blanc and Cleveland, 1968), we derive a range of values for the cells in old deposits—by using recent failures to model within-slide susceptibility (S_{IS}) as a variant of that between deposits (S).

To prepare the statistical map of susceptibility we divided the land portion of the Oakland study area into 969,003 rectangular cells 30 meters on a side, corresponding to spacing of the gridded elevation array (Graham and Pike, 1997, 1998a), and created a series of constituent raster-grid maps at this resolution. The digital maps are of geology, presence or absence of old landslide deposits, ground slope, and a point-location sample of documented post-1970 landslides. Similar digital maps were compiled for the adjacent Niles quadrangle, where the lithology is similar to that in the study area, to test the susceptibility model. Calculations were carried out in the GRID module of version 7.1.2 of ARC/INFO, a commercial GIS, on a SUN/Solaris UNIX computer, using a two-step algorithm written in Arc Macro Language.

INPUT TO THE SUSCEPTIBILITY MODEL

Geology

Hillside materials are a major, if not the dominant, site control over the larger and deeper types of slope failure worldwide (Pachauri and Pant, 1992; Mora and Vahrson, 1994; Hylland and Lowe, 1997; Cross, 1998; Massari and Atkinson, 1999; Irigaray and others, 1999; Dhakal and others, 2000). In the San Francisco Bay region, the varied prevalence of landsliding with rock type and geologic structure is well documented (Cleveland, 1971; Brabb and others, 1972; Nilsen, Taylor, and Dean, 1976; Bechini, 1993; Haydon, 1995). This control is evident in the greater Oakland area (table 1), for example, where landslides are conspicuous in two major geologic units with high clay content, the Miocene Orinda (Tor) and Briones (Tbr) Formations, but rare in two other major units, the Cretaceous Oakland Conglomerate (Ko) and the Redwood Canyon Formation (Kr) (Radbruch and Case, 1967; Radbruch, 1969; Keefer and Johnson, 1983; Bechini, 1993).

The map area is underlain by 120 diverse lithologic units. Figure 2 (on map), a 36 km^2 region within the Oakland East quadrangle, exemplifies the complex geology. The data on which our model is based are from a new digital database of revised geology, compiled at 1:24,000 scale, that integrates the published and unpublished maps of prior workers with new mapping and field checking (Graymer, 2000). Rocks of the uplands in and east of Oakland comprise 100 bedrock units occupying 62 percent of the study area. They belong to several large fault-bounded blocks that contain unique stratigraphic sequences of typically middle-upper Mesozoic to upper Tertiary sedimentary rocks (Graymer, 2000). The 100 hillside units (including the 10 that are queried in table 1) range in areal extent from less than 0.01 km^2 (Tbgl, limestone member of the middle-upper Miocene Briones Formation) to 90 km^2 (Tus, unnamed upper Miocene sedimentary and volcanic rocks). Old landslides occur so widely in these 100 hillside formations that their deposits are mapped in all except eight small units. Of these eight units only one (fg, Franciscan Complex greenstone) occupies more than 450 30-m grid cells (table 1). The 20 geologic units (one is queried) that are unconsolidated Quaternary deposits comprise 38 percent of the study area, largely in flatland terrain, and contain few old landslides (table 1). Only five of these 20 units host old failures: alluvial fan and fluvial deposits (Qpoaf, Qpaf, and Qhaf), Holocene stream channel deposits (Qhsc), and artificial fill (af).

Old Landslide Deposits

Evidence of past landsliding often is cited as an indicator of future movement in the Bay region (Cleveland, 1971; Nilsen, 1973a, b; Nilsen and Turner, 1975; Wieczorek, 1984; Haydon, 1995; Keefer and others, 1998). Our susceptibility model is based on an inventory of over 6,700 landslide deposits compiled within the Project Impact area by T.N. Nilsen (Nilsen, 1973a, b; Nilsen, 1975). Figure 3, on map, the same sub-area in the Oakland East quadrangle as figure 2, shows part of this inventory. Nilsen mapped deposits, exclusive of the difficult-to-identify upslope crowns and head scarps, at 1:24,000 scale by reconnaissance stereointerpretation of aerial photographs, the most recent of which were taken in 1968 at scales of 1:20,000 and 1:30,000. Because slope processes, especially for older landslides, are not interpreted reliably from aerial photographs alone none of the deposits are attributed by type of movement (Varnes, 1978) or causal agent (rainfall- versus earthquake-induced). Nor were landslide identifications verified by field checking. Detailed, fine-scale maps that report the mode of failure for every slide mapped are rare in the San Francisco Bay region and cover very small areas (Radbruch and Weiler, 1963; Wieczorek, 1984). More recent 1:24,000-scale map inventories cover some of the study area but lie outside the Oakland and Berkeley city limits (Haydon, 1995; Majmundar, 1996a, b).

Table 1. Geologic units, old landslide deposits, and post-1970 landslides — arrayed by spatial frequency

GEOLOGIC UNIT			OLD LANDSLIDE DEPOSITS		POST-1970 LANDSLIDES	
Map symbol	Name (after Graymer, 2000)	All cells (number of 30-meter grid cells)	Landslide cells (number of grid cells)	Spatial frequency (Landslide cells / All cells)	Total number (one grid cell per landslide)	Number on old landslide deposits
Kfa	Franciscan Complex - Alcatraz terrane	1002	820	***0.82***	6	6
Tn?	Neroly Sandstone ?	1786	1120	***0.63***	2	2
Tc	x Cierbo Sandstone	70	40	***0.57***	0	0
Th?	Hambre Sandstone ?	2514	1428	***0.57***	1	0
KJfsp	Franciscan Complex serpentinite	2596	1453	***0.56***	8	6
Tst	Siesta Formation - mudstone	5862	2937	***0.50***	6	3
Tshc	shale and claystone (Eocene)	6800	3306	***0.49***	2	2
Tbgc	x Briones Fm - conglomerate (Miocene)	119	55	***0.46***	0	0
Tmls	x Mulholland Fm - sandstone marker beds	75	33	***0.44***	0	0
Tr?	x Rodeo Shale ?	30	12	***0.40***	0	0
Tusl	x unnamed sed., volc. rocks - sed. rx mapped locally	49	19	***0.39***	0	0
Tus	unnamed sed. and volc. rocks (late Miocene)	99233	35956	***0.36***	178	37
KJfy	Franciscan Complex - Yolla Bolly terrane	1589	555	***0.35***	19	7
Tbd	Briones Fm - massive, med. ss w/ conglomerate	3261	1039	***0.32***	0	0
sc	x Si-carbonate, altered serp. - Coast Range ophiolite	77	24	***0.31***	1	0
Tul	x unnamed limestone (Miocene and Pliocene)	29	9	***0.31***	0	0
Tccs	x Claremont Shale - interbedded sandstone	239	72	***0.30***	0	0
Tms	Moraga Formation - sandstone	2797	837	***0.30***	12	3
Tbi	x Briones Formation - feldspathic sandstone	67	20	***0.30***	0	0
Tmll	Mulholland Formation - lower	18812	5518	***0.29***	85	15
Ts?	x Sobrante Sandstone ?	304	88	***0.29***	0	0
Tmlu	Mulholland Formation - upper	14578	4158	***0.29***	70	12
Tor	Orinda Formation (Miocene)	35166	9682	***0.28***	83	27
Tvhu	Vine Hill Sandstone - upper member (ss and shale)	996	270	***0.27***	0	0
Tbr	Briones Formation - ss, slt, cgl, shell breccia	32548	8723	***0.27***	29	5
Tvh	Vine Hill Sandstone	1047	272	***0.26***	3	0
Tt?	Tice Shale ?	1646	405	***0.25***	1	0
Tbp	Bald Peak Basalt	1457	356	***0.24***	0	0
Tbh	Briones Formation - Hercules Shale Member	1954	446	***0.23***	0	0
To?	Oursan Sandstone ?	477	108	***0.23***	0	0
sp	serpentinite - Coast Range ophiolite	3183	720	***0.23***	13	5
Tbu	Briones Fm - upper sandstone and shale member	8564	1814	***0.21***	0	0
Tm	Moraga Formation	6401	1345	***0.21***	5	0
KJfm	Franciscan Complex mélange - undivided	12212	2559	***0.21***	66	19
Tss	x unnamed ss. (upper Miocene and (or) Pliocene)	112	23	***0.21***	0	0
Tbl	Briones Fm - lower sandstone, siltstone member	7517	1510	***0.20***	0	0
Tmb	Moraga Formation - basalt	8231	1516	***0.18***	14	2
Tts	x tuffaceous sandstone (Oligocene or Miocene)	179	32	***0.18***	0	0
Tr	Rodeo Shale	9362	1626	***0.17***	8	1
Tbg	Briones Fm - massive ss, pebble cgl, shell breccia	12729	2167	***0.17***	1	1
Tbf	Briones Fm - feldspathic ss and brown shale	2541	432	***0.17***	0	0
Tro	Rodeo Sh, Hambre SS, Tice Sh, Oursan SS - undiv.	5294	895	***0.17***	0	0
Tt	Tice Shale	4001	632	***0.16***	1	0
Jgb	x gabbro and diabase - Coast Range ophiolite	19	3	***0.16***	0	0
To	Oursan Sandstone	5489	860	***0.16***	4	1
Tcs	Claremont Shale - chert and siliceous shale	3602	502	***0.14***	2	0
Th	Hambre Sandstone	26341	3454	***0.13***	7	0
Tsm	unnamed glauconitic mudstone	3389	438	***0.13***	24	0
KJkc	Knoxville Formation - pebble-cobble conglomerate	1580	204	***0.13***	2	1
Tlt	x tuff at Lafayette of Wagner (1978)	434	56	***0.13***	0	0
Kcs	Great Valley sequence - gray massive qtz. arenite	861	111	***0.13***	0	0
Tsr	x San Ramon Sandstone	440	56	***0.13***	0	0
Tsms	x unnamed glauconitic mudstone - siltstone and ss	362	46	***0.13***	3	0
Tn	Neroly Sandstone	23440	2753	***0.12***	13	1
Tvhl	Vine Hill Sandstone - lower member (glauconitic)	2389	279	***0.12***	1	0
Ts	Sobrante Sandstone	5987	689	***0.12***	0	0
Tcc	Claremont Chert	10590	1177	***0.11***	4	0
Jpb?	x pillow basalt, basalt breccia, and minor diabase ?	145	15	***0.10***	0	0
Ksh	Great Valley sequence - siltstone and shale	459	47	***0.10***	0	0
Tes?	x Escobar Sandstone (Eocene) ?	146	14	***0.10***	1	0
Ksc	Shephard Creek Formation	5675	508	***0.09***	12	1
Tub	x unnamed basalt (Miocene and Pliocene)	34	3	***0.09***	0	0
KJk	Knoxville Formation	8164	663	***0.08***	25	1
Kus	Great Valley sequence - ss., siltstone, shale	7855	631	***0.08***	1	1

Table 1. Geologic units, old landslide deposits, and post-1970 landslides — Continued

GEOLOGIC UNIT			All cells (number of 30-meter grid cells)	OLD LANDSLIDE DEPOSITS: Landslide cells (number of grid cells)	OLD LANDSLIDE DEPOSITS: Spatial frequency (Landslide cells / All cells)	POST-1970 LANDSLIDES: Total number (one grid cell per landslide)	POST-1970 LANDSLIDES: Number on old landslide deposits
Map symbol		Name (after Graymer, 2000)					
Jsv		keratophyre, qtz. keratophyre above ophiolite	15627	1212	*0.08*	50	6
Tbe		Briones Fm - med. ss w/ shell breccia	3922	304	*0.08*	0	0
Qpoaf	Q	older alluvial fan deposits (Pleistocene)	6482	499	*0.08*	26	7
Ku		Great Valley sequence - undifferentiated	12706	965	*0.08*	35	2
Tmu		mudstone, shale and siltstone (Miocene)	635	48	*0.08*	1	0
Kp		Pinehurst Shale	554	40	*0.07*	0	0
Tsa		sandstone (Miocene)	1243	78	*0.06*	1	0
Kr		Redwood Canyon Formation (Cretaceous)	27503	1697	*0.06*	27	1
Tes		Escobar Sandstone (Eocene)	2513	141	*0.06*	43	3
KJkv	x	Knoxville Formation - volcanoclastic breccia	209	11	*0.05*	0	0
Tush		unnamed gray mudstone (early Miocene)	861	36	*0.04*	0	0
Tdi		diatomite (Miocene)	1942	79	*0.04*	1	0
Tgvt		Green Valley Tonalite, Tassajara Fm - undivided	10463	388	*0.04*	5	0
Tuc	x	unnamed conglomerate (Miocene)	195	7	*0.04*	2	0
fs		Franciscan Complex sandstone	3441	109	*0.03*	9	1
Tmru	x	Muir Sandstone - upper member	229	7	*0.03*	1	0
Tcgl		Garrity unit (Wagner) - cgl, ss, siltstone	11293	343	*0.03*	31	0
Jpb		pillow basalt, basalt breccia, and minor diabase	2727	79	*0.03*	0	0
Kcv		unnamed sandstone, conglomerate, and shale	18167	453	*0.02*	1	1
gb		gabbro - Coast Range ophiolite	10495	250	*0.02*	25	1
Jb		massive basalt, diabase - Coast Range ophiolite	1572	35	*0.02*	6	0
KJf		Franciscan Complex - undivided	755	15	*0.02*	9	0
Ta	x	unnamed glauconitic sandstone	163	3	*0.02*	4	0
Kc		Great Valley seq. - pebble-boulder conglomerate	1110	19	*0.02*	0	0
Qpaf	Q	alluvial fan and fluvial deposits (Pleistocene)	61867	1010	*0.02*	87	0
Kfn		Franciscan Complex - Novato Quarry terrane	7879	122	*0.02*	27	1
Kss	x	Great Valley sequence - unnamed ss. (Cret.)	66	1	*0.02*	0	0
Ko		Oakland Conglomerate (Cretaceous)	20921	301	*0.01*	6	0
Kjm		Joaquin Miller Formation	20872	258	*0.01*	22	1
Qhsc	Q	stream channel deposits (Holocene)	5199	39	*0.01*	7	0
fc	x	Franciscan Complex chert	323	1	*0.00*	0	0
Qhaf	Q	alluvial fan and fluvial deposits (Holocene)	125014	254	*0.00*	38	0
af	Q	artificial fill (Historic)	65934	15	*0.00*	5	0
Qpaf1	Q	alluvial terrace deposits (Pleistocene)	369	0	*0.00*	0	0
alf	Q	artificial levee fill (Historic)	2344	0	*0.00*	0	0
Qhasc	Q	artificial stream channels (Historic)	626	0	*0.00*	0	0
Qhb	Q	basin deposits (Holocene)	26485	0	*0.00*	0	0
Qhbm	Q	bay mud (Holocene)	7613	0	*0.00*	0	0
Qhbr	Q	beach ridge deposits (Holocene)	85	0	*0.00*	0	0
Tbgl	x	Briones Formation - limestone	11	0	*0.00*	1	0
Tccs?	x	Claremont Shale ? - interbedded sandstone	19	0	*0.00*	0	0
Qhds	Q	dune sand (Holocene)	9043	0	*0.00*	0	0
Qhbs	Q	floodbasin deposits (salt-affected) (Holocene)	531	0	*0.00*	0	0
Qhfp	Q	floodplain deposits (Holocene)	9092	0	*0.00*	0	0
fg		Franciscan Complex greenstone	730	0	*0.00*	0	0
Kfgm	x	Franciscan Complex quartz diorite intrusive	175	0	*0.00*	0	0
KJfs	x	Franciscan Complex sandstone - undivided	326	0	*0.00*	8	0
Tcglt	x	Garrity unit (Wagner), rhyolite tuff, tuff breccia	63	0	*0.00*	0	0
Kslt	x	Great Valley sequence - unnamed siltstone	314	0	*0.00*	1	0
QTi?	Q	Irvington Gravels ? (Pleistocene)	60	0	*0.00*	0	0
Qmt	Q	marine terrace deposits (Pleistocene)	2890	0	*0.00*	0	0
Qhms	Q	Merritt Sand (Holocene)	7911	0	*0.00*	0	0
Qhl	Q	natural levee deposits (Holocene)	31057	0	*0.00*	0	0
sp?	x	serpentinite ? - Coast Range ophiolite	42	0	*0.00*	0	0
QTu	Q	surficial deposits, undif. (Pliocene-Pleistocene)	342	0	*0.00*	0	0
Qhaf1	Q	younger alluvial fan deposits (Holocene)	1086	0	*0.00*	0	0
water	†	inland water - reservoirs and streams	111,717	124	*0.00*	0	0
		Total (reservoirs and streams excluded)	**969,003**	**116,360**	***‡ 0.12***	**1192**	**183**

† Water excluded; 124 landslide cells on water result from minor mismatches between base map and landslide-deposit inventory

x Hillside units with fewer than 450 cells; distributions of Landslide cells/All cells (fig. 6) are less regular than other units'

Q20 Quaternary units in flatland terrain; most are less susceptible to landsliding than hillside units (the 100 remaining entries)

‡ Mean spatial frequency of old landslide deposits for entire study area

Nilsen identified landslide deposits on the basis of landscape features known to characterize the various types of failure (Liang and Belcher, 1958; Ritchie, 1958). Among these features are (1) small isolated ponds, lakes, and other closed depressions; (2) abundant natural springs; (3) abrupt and irregular changes in slope and drainage pattern; (4) hummocky and irregular surfaces; (5) smaller, younger landslide deposits that form within older, larger deposits; (6) steep, arcuate scarps at the upper edge of the deposit; (7) irregular soil and vegetation patterns; (8) tilted trees and other signs of disturbed vegetation; and (9) abundant level areas within steep slopes. Nilsen (1973a, b) noted fewer of these characteristics in smaller deposits. Complex landslide masses, resulting from combinations of different styles of downslope movement, are perhaps the most common type mapped. Deposits varied in appearance from clearly discernible, unweathered and uneroded topographic features to indistinct, highly weathered and eroded forms recognizable only by characteristic topographic configurations. Many medium-size and all of the largest slide masses had coalesced from smaller deposits that Nilsen (1973a) did not identify individually. Coalesced slides were mapped as one deposit and are so treated here. Finally, because Nilsen mapped landslide deposits remotely and not all of his identifications were definitive, he ascribed two levels of confidence to his interpretations. Deposits were queried where identification was uncertain.

We compiled Nilsen's (1973a, b) landslide deposits as a digital database. His original linework inked on 1:24,000-scale Mylar greenlines (Nilsen, 1975) was scanned (400 dots per inch), converted automatically from raster to vector form, imported into ARC/INFO, edited to remove all information except landslide polygons, and combined into one file. The paper-map inventory had not been wholly edge-matched. Where needed, we adjusted landslide-deposit outlines to align across adjacent quadrangles. The few deposits designated by Nilsen as "identification uncertain", and so indicated in the database and by a different color on derivative maps (Roberts and others, 1999), were not treated differently. Because landslide inventories are inherently incomplete, our inclusion here of false positives—Nilsen's identifications, both certain and uncertain, that are not landslide deposits (T. McCrink, personal communication, 2000)—is more likely to make up the deficiency of other deposits missed by Nilsen than to exaggerate or otherwise misrepresent the true extent of slope failure.

Table 2. Prevalence of old landslide deposits, by type of land use†

Land-use category	Number of slide deposits	Percentage of each land-use category that is slide deposit *
Forest land	3197	18 %
Rangeland	2246	26
Residential land	935	10
Vacant & mixed-urban open	217	8
Commercial	27	4
Education	26	5
Wetland	24	5
Infrastructure	13	3
Agriculture	8	3
Industrial	7	7
Extensive outdoor recreation	7	16
Sparsely vegetated	5	8
Military	2	5
Mixed residential-commercial	0	2
Mixed residential-industrial	0	2
Public institutions	0	1
Hospitals	0	0

† Association of Bay Area Governments (1996)
* limited to area most likely to fail—above 90m elevation and 10° slope

Nilsen's data well represent the extent of prior landsliding in the Project Impact area, despite errors in his inventory and its dissimilarities with other mapping. In addition to the operational constraints of time and airphoto availability, quality, scale, date, and season, landslide inventories are sensitive to variance in mapper experience and personal idiosyncrasies. The topographic expression of unstable slopes is complex and subtle, and not all mappers apply the same criteria or interpret them similarly. Some observers map both the landslide scar and the deposit rather than only the deposit; others excel at recognizing landslides only in certain types of bedrock, terrain, or vegetative cover. These factors result in different inventories of the same area by different mappers. To compare such differences numerically, we made a GIS analysis of the landslide-deposit inventories by Nilsen (1975) and Majmundar (1996b) for the Las Trampas Ridge quadrangle (fig. 1).

(This is not intended as an unbiased test; Majmundar used Nilsen's map and had later photos.) Nilsen mapped 48 km^2 of landslide deposits and Majmundar 39 km^2, of which 35 km^2 overlap. Nilsen thus included 90 percent of the total area mapped by Majmundar plus another 13 km^2, whereas Majmundar included 72 percent of Nilsen's total area plus an added 4 km^2. Of the 2,196 individual deposits identified by Nilsen, 1,933 (88 percent) coincide at least partially with one of the 1,803 mapped by Majmundar, whereas 1,708 (95 percent) of Majmundar's deposits coincide with one of Nilsen's.

The 6,714 mapped landslide deposits occupy 12 percent of the study area, and 320 of them lie within the Oakland city limit. Most landslides are in hills to the northeast, cover 19 percent of this upland area (defined as the 100 non-Quaternary units in table 1), and cluster in elongate patterns that align with the regional NW-SE topographic trend. The deposits vary in size from about 1,100 m^2 to 4 km^2 and from 60 m to 5 km in the longest dimension for the largest of the many coalesced masses, although most are less than 100 m long (fig. 3). Individual deposits range widely in average ground slope (2° to 44°; mean approximately 20°) and shape, complexity of planimetric form tending to increase with size from ellipses to convoluted outlines. Estimated times of initial movement are uncertain and vary from 35 years to 100,000's of years before present, although elevated precipitation in the late Pleistocene has been hypothesized for smaller, shallow landslides in the San Francisco Bay area (Reneau and others, 1986). Some slide deposits moved or continue to move over long periods, and many large masses host smaller recent landslides. The presumed types of movement, translational and rotational block slide and earthflow, and contributing causes of instability, rainfall and seismic shaking, are undetermined for individual landslide deposits.

Many past slope failures underlie areas of present human occupancy or land likely to be developed. Although 81 percent of the 6,714 landslide deposits in the study area are located in forest and rangeland (much of it in parks) and thus pose a limited present or potential hazard, 935 deposits occupy approximately 15 percent of all residential areas (as of 1995) and at least 75 additional deposits occur in other urban areas (table 2). The landslides in residential areas occupy 10 percent of the region we believe most prone to instability, terrain above an elevation of 90 m and a slope of 10°.

Recent Landslides

Portions of old landslide deposits in the San Francisco Bay region often are destabilized by earthquake (Keefer and others, 1998) or heavy rainfall (Pike and others, 1998). Barring a return to the climatic conditions under which they formed, perhaps in the late Pleistocene (Reneau and others, 1986) or an earlier glacial-nonglacial transition, most large old slides that were triggered by high rates of precipitation are unlikely to again move in their entirety. Smaller deposits and parts of large masses, however, frequently remobilize (Nilsen, Taylor, and Dean, 1976; Keefer and Johnson, 1983; Baum and others, 1998; Jayko and others, 1998), and for the purpose of hazard recognition should be considered dormant rather than relict (extinct). Accordingly, old landslide deposits commonly are judged more susceptible to future movement than are unfailed areas of comparable slope that lie outside them (Nilsen and Wright, 1979; Cotton and Cochrane, 1982; Wieczorek, 1984; Haydon, 1995). This potential for added risk needs to be incorporated into susceptibility estimates. The magnitude of risk is difficult to determine, but can be approximated from the occurrence of recent movements within the older slides.

Although landsliding remains common throughout the Project Impact area, the only available data from which to modify within-slide susceptibility are 1,192 post-1970 rainfall-induced failures that damaged the built environment. The 1,192 landslides are recorded in 1:62,500-scale maps by Nilsen and Turner (1975) and Nilsen, Taylor, and Brabb (1976); unpublished information compiled by F.A. Taylor in the 1970's; and post-1998 El Niño observations for Alameda and Contra Costa Counties (Coe and others, 1999; Graymer and Godt, 1999)—931, 105, and 156 landslides, respectively. Because outlines of most of these failures were not recorded, their locations were compiled digitally as point data and assigned to the center of the nearest 30-meter cell (fig. 3). Of the 1,192 post-1970 landslides, 183 (15 percent) reactivated older deposits mapped by Nilsen (1975).

Distribution of the 1,192 recent slides among the 120 geologic units largely mimics the varied prevalence of old landslide deposits (table 1), a consistency we judge sufficient for these recent data to be used in the model. Although more of the post-1970 landslides are recorded in the larger units, which suggests some role of chance in their occurrence, table 1 shows that the pattern of slope instability is not random. Thirty-six geologic units have six or more recent failures. Of these 36 units, the five bedrock formations that host the largest numbers of post-1970 slides (totaling 40 percent of the 1,192 failures) all have high mean frequencies (>0.20) of old slide deposits (table 1): the widespread unnamed unit Tus (n=178 recent slides), upper and lower members of the Mulholland Formation (Tmll, n=85 slides; Tmlu, n=70), the Orinda Formation (Tor, n=83), and undivided Franciscan Complex mélange (KJfm, n=66). These five susceptible hillside units, moreover, contain 60 percent of the 183 post-1970 failures that also occur in old landslide masses (see table 1). Similarly, the three Quaternary flatland units that recorded the highest numbers of post-1970 failures—younger Pleistocene alluvial fan deposits (Qpaf, n=87 slides), older Pleistocene alluvial fan deposits (Qpoaf, n=26), and Holocene alluvial fan deposits Qhaf (n=38)—also are the three surficial units that have the most area in old landslide deposits (≥250 cells per unit; see table 1). Table 1 reveals further that only seven of the 183 recent slides that also occur on old slide deposits are in Quaternary geologic materials, all in Qpoaf, the most susceptible Quaternary unit. Recent failures tend to be rare in the geologic units that contain the fewest old landslide deposits; none of the 28 units in table 1 that have six or fewer cells on old landslide masses hosted any post-1970 failures.

The 1,192 recent landslides, which damaged road cuts, graded fill, and other manmade works (Nilsen and Turner, 1975, p. 6-7), are not ideal data to use in modeling within-slide susceptibility, for in several

respects they little resemble the slide deposits mapped previously. These post-1970 landslides (many of which include scarps and crowns in addition to their deposits) are much smaller than most of the old slide masses mapped by Nilsen, none was generated by earthquake, the positional accuracy of those located from broad-scale maps exceeds the 30-m size of the grid cells, and—most important—the true incidence of fresh failures within old landslide deposits cannot be known because of an anthropogenic bias: hillside development increases the susceptibility of normally stable geologic materials to slope failure.

The 1,192 damaging post-1970 landslides are failures of cut-and-fill grading in urbanized areas, many of them in such otherwise safe materials as alluvial fan (Qpaf, Qhaf, and Qpoaf; n=151 slides), the Garrity unit (Tcgl, n=31), and the Novato Quarry terrane (Kfn, n=27). (Note the spatial coincidence of recent slides with local roads in unit Kfn in figure 3.) Table 1 shows that of the 1,192 recent landslides only 675 occurred in the 60 more-susceptible units (those with >10 percent of area in old landslide deposits), whereas 517 were in the 60 less-susceptible units (< 10 percent area in old deposits). Moreover, only 15 percent (n=183) of the recent failures occurred in the pre-1970 landslide deposits mapped by Nilsen; the remaining 1,009 were in terrain that had not moved previously, including Quaternary materials. These 1,009 post-1970 slides thus overrepresent both the urbanized lowland bordering the Hayward Fault and developed parts of the adjacent hills (fig. 4, on map). An unbiased sample, which would include the many non-damaging (but currently unmapped) recent failures in the undeveloped uplands east of Oakland, would require a substantial effort toward which resources have yet to be directed by public agencies.

Topography and Slope

Configuration of the land surface (fig. 4) is related to the processes that continue to shape San Francisco Bay region hillsides (Radbruch and Weiler, 1963; Cleveland, 1971; Waltz, 1971; Nilsen, Taylor, and Dean, 1976; Nilsen and Wright, 1979), as well as other areas worldwide (Mora and Vahrson, 1994; Massari and Atkinson, 1999; Irigaray and others, 1999). So diagnostic to the expert observer is the topographic expression of all but the oldest landslide deposits (see list of features above, under Old Landslide Deposits), that the extent of much past failure can be identified from a visual appraisal of the terrain at scales as coarse as 1:30,000 (Brabb and Pampeyan, 1972; Nilsen, 1973a, b). Few of the geomorphic features that characterize a landslide or tract of landslide-prone terrain (Liang and Belcher, 1958; Ritchie, 1958) translate readily into measures, parameters from which a numerical index of susceptibility can be computed. Among these few measures is surface gradient, or slope, the first derivative of elevation with respect to the horizontal and arguably the single most important descriptor of ground-surface form (Evans, 1972; Pike, 1988). The relation between slope and landsliding is complex (Lanyon and Hall, 1983; Wentworth and others, 1987; Pike, 1988; Dietrich and others, 1993; Montgomery and Dietrich, 1994). To evaluate the role of topography in landsliding in the Project Impact area, we calculated slope for each 30-m grid cell.

Our data are from a recent slope map of the 10-county San Francisco Bay region computed from a digital elevation model (DEM), a rectangular matrix of terrain heights spaced at a constant interval (Graham and Pike, 1998b). Slope, in one-degree increments, is the maximum rate of change for the central 30-m cell within each 3 × 3 subgrid of cells. The full San Francisco Bay region set of about 35,000,000 cells was assembled from 204 smaller DEM's derived from individual 7.5' quadrangles (Graham and Pike, 1997, 1998a). The 7.5' DEM's were created by interpreting elevations from map contours (U.S. Geological Survey, 1993) rather than by prior, less accurate, techniques. Accordingly, the new DEM is free of the striped artifacts that marred shaded-relief portrayals and generated erroneous analyses from older 30-m data (Graham and Pike, 1997). However, the source contours portray topography mapped from the late 1940's to the early 60's, before much of the subsequent residential development (Stromberg, 1967); the DEM does not capture the myriad cut-and-fill changes that have since altered many of the local hillsides and thereby increased their potential susceptibility to failure. (We discuss possible implications of this problem later in the report.) Because it is derived from the same contour maps, a newer 10-m USGS DEM of the region does not increase the detail relevant to our susceptibility model over that in the 30-m data, although it yields a smoother-appearing shaded-relief image (fig. 4) of the sample area in figures 2 and 3.

The slopes of failed and unfailed terrain in the study area differ dramatically, as shown by the histograms in figures 5A and B. Slopes on old landslide deposits are near-normally distributed (fig. 5B) and peak at about 16°-17°, whereas unfailed slopes (fig. 5A) are strongly skewed toward low values, with the mode at zero. Much of this contrast reflects the widespread coastal flatlands that hosted few old landslides. The distribution of slope for the 1,192 cells that hosted recent landslides (fig. 5C) has the same near-normal shape as that for cells on the old deposits in figure 5B, although the mode (approximately 12°) is lower by about 4°. Figures 5A and B do not express the exact relation between slope and prior landsliding, however, because Nilsen (1973a, b) did not identify the entire area affected by each old failure. The steeper slopes on terrain occupied by landslide crowns and head scarps upslope of the deposits are not included in figure 5B, which would otherwise extend to higher slope values. The magnitude of this deficiency is unknown, and we propose no arbitrary correction. The missing steep slopes must affect both the derivative histograms in figure 6 and the susceptibility map; this undersampling of older steep ground that failed (scarps) infers too low a susceptibility for all steep terrain, not just terrain upslope from mapped deposits.

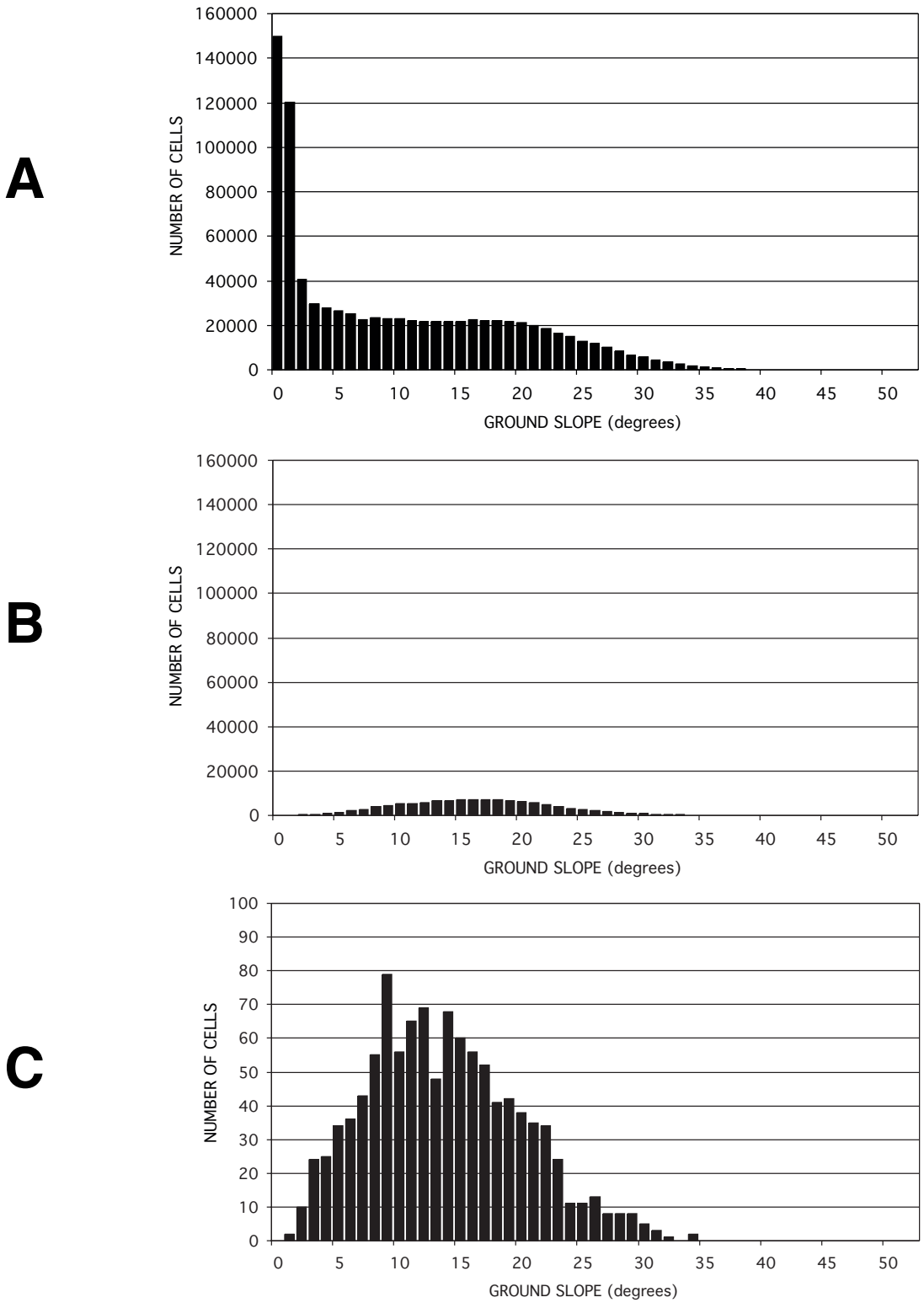

Figure 5. Distribution of ground slope in the Oakland Project Impact area shown by histograms of 30-m grid cells. A, stable terrain that has not failed. B, terrain underlain by old landslide deposits. C, terrain underlying recent (post-1970) landslides that damaged the built environment (fig. 3).

A MODEL OF LANDSLIDE SUSCEPTIBILITY

Spatial Frequency of Prior Failure

Overall susceptibility of a geologic unit to slope failure can be expressed numerically as the percentage of the unit's area that falls within existing landslide deposits (Brabb and others, 1972). This percentage, or average spatial frequency, is highly variable. Computed in table 1 as the number of 30-m cells in landslide deposits divided by all cells in the geologic unit, spatial frequency in the Oakland area ranges from 82 percent (820 of 1002 cells) in the Alcatraz terrane (Kfa), a subunit of the Franciscan Complex, to less than 1 percent in 26 different units. The more susceptible formations are among the 100 bedrock units in the greater Oakland hills; the unconsolidated Quaternary units are far less susceptible. Twenty-seven hillside units, covering one-fourth of the area, each are at least one-fourth in landslide deposits and thus quite likely to host slopes that will mobilize in the future. By contrast, less than one percent of the area underlain by the 20 Quaternary flatland units in table 1 is on landslide masses (1,817 of 364,030 cells, mostly in the widespread younger Pleistocene alluvial fan deposits Qpaf). The highest spatial frequency of landslide deposits among Quaternary units occurs in Qpoaf, older Pleistocene alluvial fan (8 percent). The 10 queried units in table 1 that have nonqueried counterparts all differ from (and eight are higher than) the nonqueried units in areal prevalence of landslide deposits, which indicates that the lithologic contrasts distinguishing queried units have real consequences with respect to potential for slope instability. Mapping the mean values of spatial frequency in table 1 alone yields a generalized map of landslide susceptibility (not shown), but its usefulness is limited by the lack of detail.

The whole-unit spatial frequencies in table 1 can be refined considerably by ground slope. Blanc and Cleveland (1968), Radbruch (1970, p. 4), Brabb and others (1972), Roth (1983), and Bechini (1993), among others, noted that prevalence (defined in various ways) of non-debris-flow landsliding in the San Francisco Bay area and elsewhere in California increases with terrain slope, but only up to a maximum value, commonly 15° to as much as 35°, depending on mode of failure and the underlying lithology. (Such forms of mass-movement as rock falls, topples, and shallow landslides occur in the steeper areas; debris-flow source areas, for example, peak at about 30° mean slope; Ellen, 1988.) Similar slope maxima are documented elsewhere (Lanyon and Hall, 1983; Jäger and Wieczorek, 1994; Brunori and others, 1996; Wójcik, 1997; Hylland and Lowe, 1997; Jennings and Siddle, 1998; Irigaray and others, 1999).

We examined in detail the correlation of spatial frequency of old landslide deposits with ground slope in the Oakland study area and found the relation systematically nonlinear. Histograms in figure 6 give five examples of what is fundamentally a near-normal distribution of slope failure. Figure 6A shows the entire Project Impact area, for which the mean spatial frequency is 12 percent. The rising segment of figure 6A, which includes well over half the grid cells that contain old landslide deposits, describes a positive correlation between landslide frequency and slope that confirms much of the predictive capability of slope observed previously. The spatial frequency of deposits departs from the area's 12 percent overall mean, increasing in one-degree increments from 0 percent at zero slope to about 23 percent at 19°. However, the prevalence of slide and earthflow deposits declines on steeper slopes, to about 8 percent at 33° and remains constant thereafter. This constancy persists only up to the highest values of slope, because of a sampling effect: the histogram becomes increasingly irregular as the number of cells diminishes with increasing slope. The few steep cells in figure 6A, for example (7, 2, and 3 cells at slopes of 44°, 48°, and 49°), yield unrealistically high frequencies, whereas slopes of 45°-47° host no deposits and thus have frequencies of zero. The true spatial frequency of old landslide deposits on the steepest slopes remains unknown, but probably is low and variable from unit to unit.

All but the 32 smallest geologic units in table 1 follow a bell-shaped relation similar overall to that in figure 6A. Figure 6D describes the most extensive unit in the study area, Tus, the unnamed late Miocene sedimentary and volcanic rocks. Figure 6D resembles figure 6A, but shows a much higher frequency of landsliding, averaging 36 percent in old deposits (table 1). Spatial frequency for unit Tus rises from 2 percent at zero slope to 43 percent at a slope of about 20° and thereafter diminishes to about 10 percent. Although frequencies for the steepest slopes in Tus vary irregularly, as they do for steep slopes in the entire study area (fig. 6A) as well as in other individual units, these few aberrant values (two at 38°) have little effect on the resulting statistics of susceptibility for this unit. Compared with unit Tus, the Hambre Sandstone (unit Th, fig. 6B) and younger Pleistocene alluvial fan (Qpaf, fig. 6C) have much lower spatial frequencies of old landslide deposits. Also, histograms for the 32 smallest units (< 450 cells) tend to be more rectangular than normal, as exemplified by the Lafayette Tuff in figure 6E (which shows the numbers of cells comprising each histogram bar). The bell-shaped distribution of spatial frequency with respect to ground slope is not unique to old landslide deposits, as shown in figure 6F, a histogram of the number-frequency of the 1,192 recent landslides with respect to slope.

The wide range of spatial frequencies in the histograms sampled in figures 6B-E confirms that the mean values in table 1 are unrepresentative of the hazard locally and thus cannot be used to model the likelihood of failure throughout a geologic unit. Accordingly, the 969,003 susceptibilities extracted from the spatial frequency of old landslide deposits were calculated to reflect the variability of these frequencies with ground slope in each of the 120 geologic units. We obtained susceptibility both between (n = 852,643 grid cells) and within (n = 116,360 cells) landslide masses in the Project Impact area (table 3). Because some of the latter values exceed 1.00, all 969,003 susceptibilities are expressed as a decimal rather than a percentage.

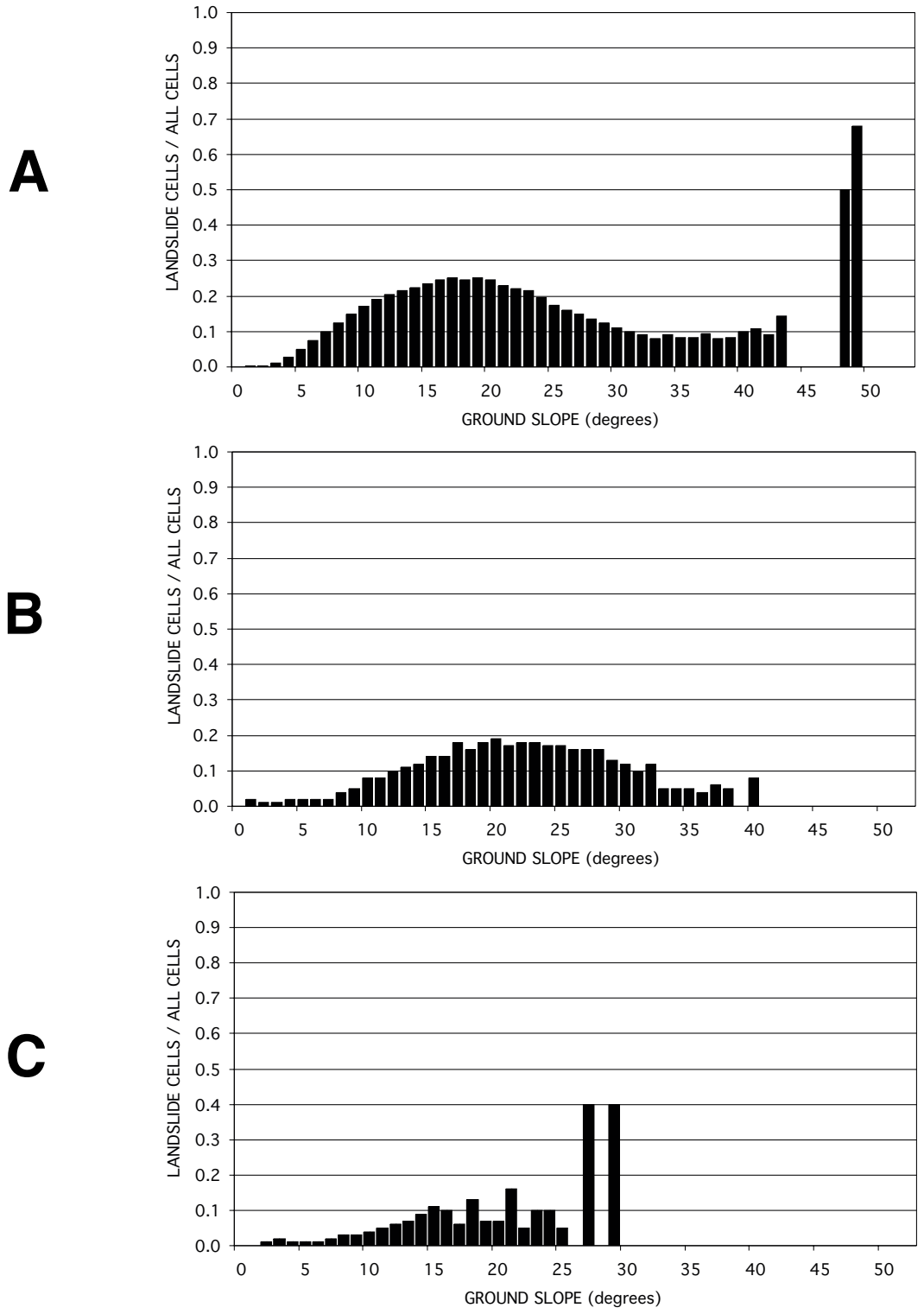

Figure 6. Spatial frequency of slope failure by sliding and earthflow, shown by ratio of number of 30-m cells on old landslide deposits to number of all cells, as a function of ground slope in 1° intervals. A, Oakland Project Impact area. B, Hambre Sandstone (map unit Th). C, Pleistocene alluvial fan deposits (Qpaf).

D

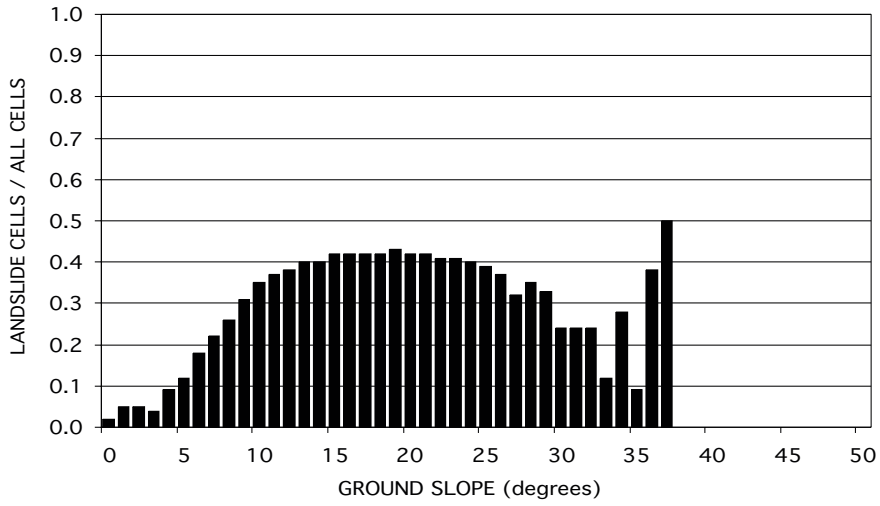

E

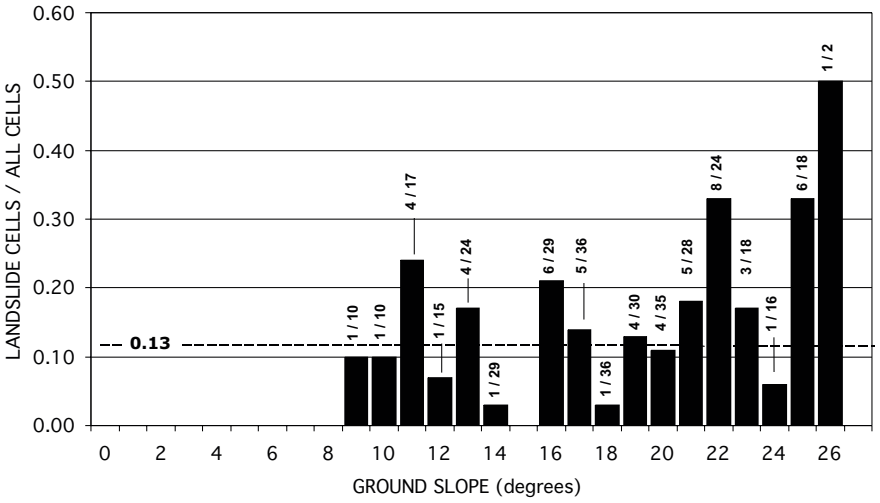

F

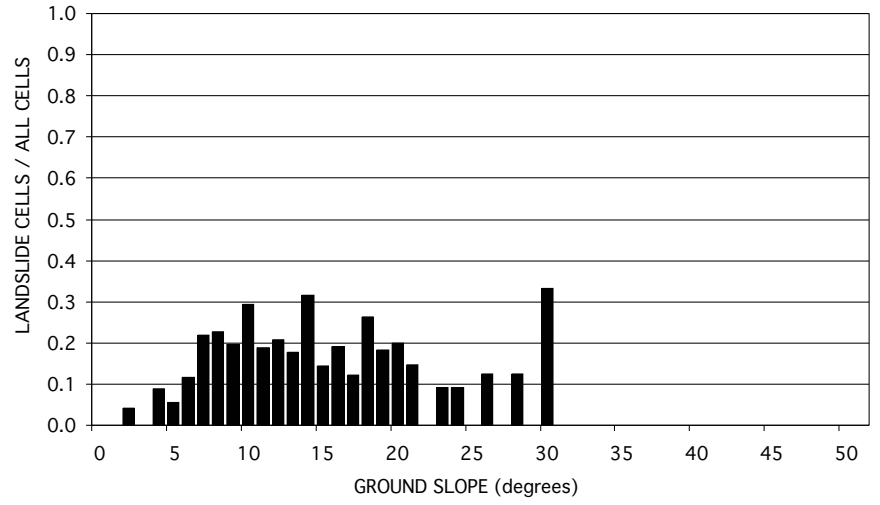

Figure 6 (continued). D, unnamed Tertiary sedimentary and volcanic rocks (Tus). E, tuff at Lafayette of Wagner (1978) (Tlt), shown at larger scale (0.13 is mean frequency; small numbers are cells for the 17 slope intervals). F, 1,192 post-1970 damaging landslides (one cell per slide). See text for discussion.

Table 3. Distribution of grid cells and their susceptibility values S_{ls} and S, by hillside or flatland sites and by location within or between old landslide deposits

Terrain and Geology	Number of 30-m grid cells*		
	All cells	S_{ls} - within slide masses	S - between slide masses
Hillsides: 100 bedrock units	604,973	114,543	490,430
Flatlands: 20 surficial units	364,030	1,817	362,213
Entire region: all 120 units	969,003	116,360	852,643

* excluding cells on inland water bodies

Susceptibility Between Old Landslide Deposits

Susceptibility S for grid cells not underlain by old landslide masses (87 percent of the study area, 81 percent of the Oakland hills, table 3) is estimated directly from the histograms that show the spatial frequency of old landslide deposits with respect to ground slope. S is calculated for each slope interval. In geologic unit Tus, for example, where 35 percent of the 30-m cells sloping at 10° are located on the old landslide masses (fig. 6D), every cell in unit Tus with a slope of 10° is assigned that same susceptibility S, of 0.35. In the less-susceptible Hambre Sandstone (unit Th, fig. 6B), by contrast, only 8 percent of the cells in the 10° slope interval lie on mapped slide masses, whereupon an S of 0.08 is assigned to all 10° cells in the Hambre. Values of S, determined slope interval-by-slope interval, are unique to each slope value in each of the 120 units. The resulting distribution of susceptibility for the 852,643 cells that lie between mapped landslide deposits is shown in figure 7A. The values are severely skewed, even in the log domain, and range from $S = 0.00$ for 300,000 cells in predominantly flat-lying surficial units to $S = 0.90$ for 14 cells in unit Kfa, Franciscan Alcatraz terrane.

Susceptibility Within Old Landslide Deposits

Obtaining susceptibility S_{ls} for the smaller fraction of the Oakland area that is underlain by landslide deposits is more complex. We first calculated raw susceptibility S for the 116,360 cells within old slide masses, by the same procedure as for cells between them. The resulting log frequency distribution (fig. 7B) has many (by 1 to 3 orders of magnitude) fewer cells in the lowest (0.00 to 0.25) S range and is more symmetric than the histogram for cells between deposits (fig. 7A). The highest value of S on landslide masses is 1.00, for 70 cells: 15 cells in unit Kfa, Franciscan Alcatraz terrane, seven or eight cells each in three small units (locally mapped sedimentary rocks, Tusl; silica-carbonate and altered serpentinite, sc; and the Cierbo Sandstone, Tc), and one to four cells each in 17 other geologic units in table 1 (not identified).

To estimate the higher susceptibilities that characterize old landslide deposits S_{ls} we raised these 116,360 values of S by a factor a, based on the spatial frequency of recent (post-1970) failures in the East Bay,

$$a = (\#\text{hist}_{ls} \ / \ A_{ls}) \ / \ (\#\text{hist}_{nls} \ / \ A_{nls}),$$

where $\#\text{hist}_{ls}$ and $\#\text{hist}_{nls}$ are the numbers of recent failures within and outside old landslide deposits, respectively, and A_{ls} and A_{nls} are the areas (in number of cells) of old deposits and the terrain between them. From this correction, (183 / 116,360) / (1,009 / 852,643) or 1.33, recent landslides in the study area are about 1/3 more likely to occur within old landslide deposits than between them. (This number differs from the 1.05 correction computed over the smaller total area in a more complex model by Pike and others, 1999a, b). In the absence of historic data on landsliding for each geologic unit, we applied the 1.33 multiplier to all units. The highest value of S_{ls} is 1.33, for the same 70 cells in unit Kfa and the 20 other units mentioned above. The shape of the resulting frequency distribution of susceptibility (fig. 7C) is essentially that for the raw S values (fig. 7B). Figure 7D combines figures 7A and 7C to yield the distribution of susceptibility for all 969,003 grid cells plotted on the map.

The 33 percent higher incidence of post-1970 landslides on old slide deposits is of the same magnitude cited previously for the East Bay, about 55 -70 percent in the more susceptible geologic units (Nilsen, Taylor, and Dean, 1976, p. 19), but may be low. Keefer and others (1998, fig. 4), for example, found that 18 of the 20 largest slides triggered in the Santa Cruz Mountains by the 1989 Loma Prieta earthquake occurred within areas that had failed previously (≥55 percent spatial overlap)—not necessarily an invalid comparison despite the difference in triggering mechanisms.

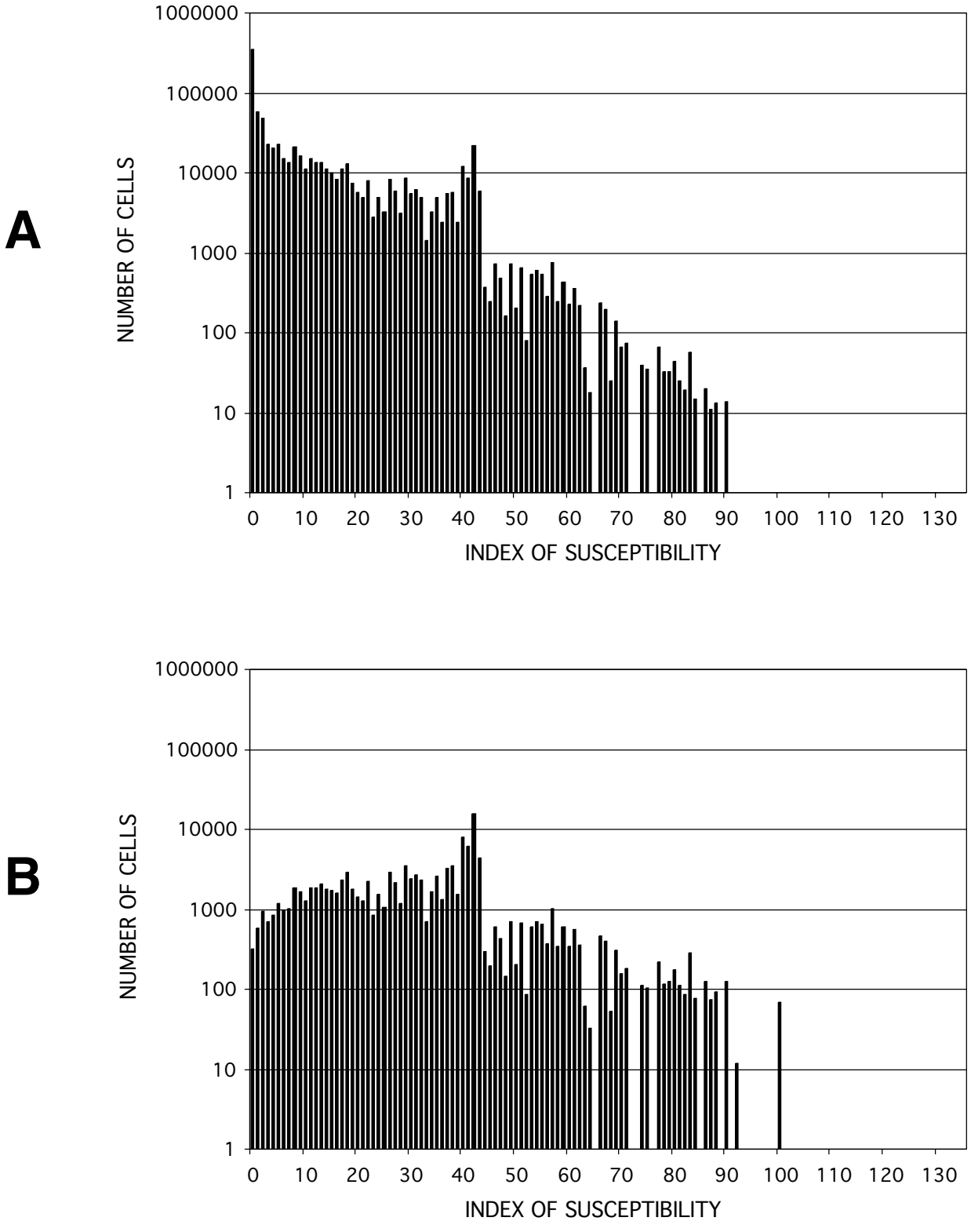

Figure 7. Distribution of susceptibility to slope failure by sliding and earthflow in the Oakland Project Impact area, shown by log number of grid cells as a function of modeled index number. A, Between old landslide deposits (*S*). B, Within old landslide deposits—uncorrected (*S*).

C

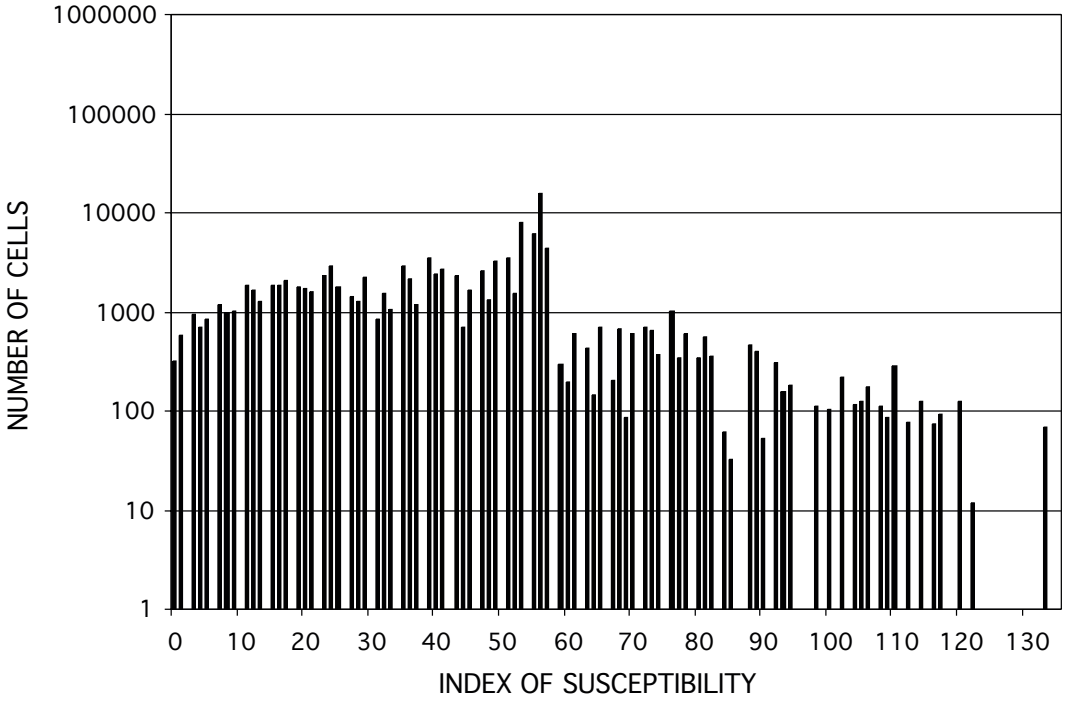

D

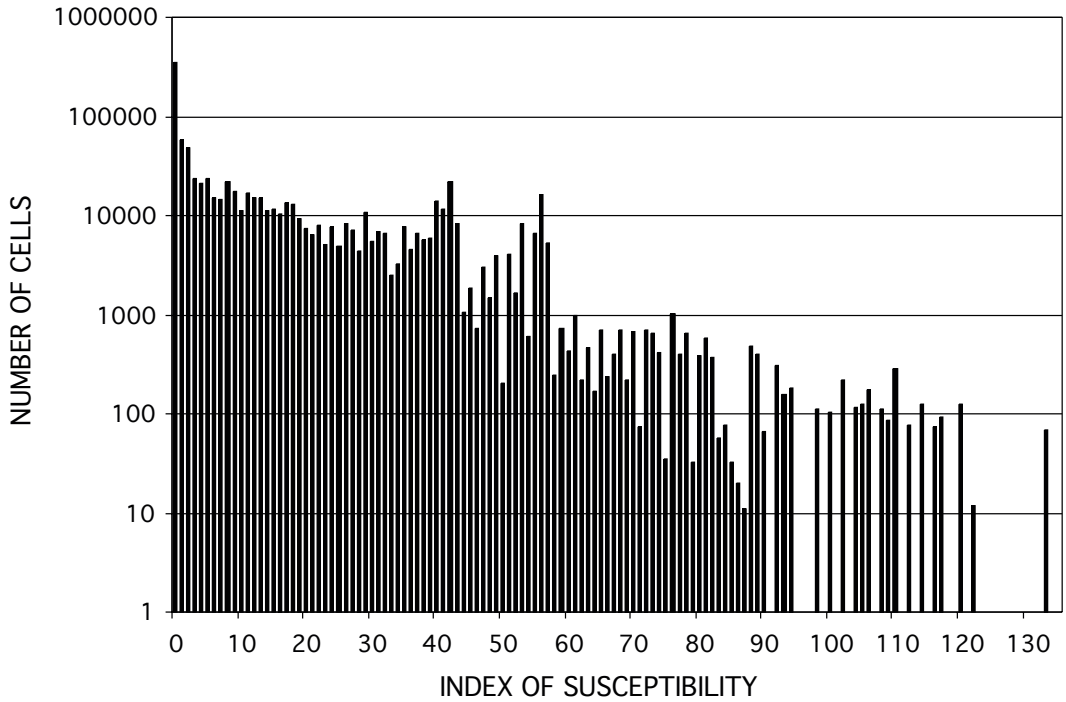

Figure 7 (continued). C, Within old deposits × 1.33 correction factor (S_{ls}). D, Final result for entire map area (A + C; $S + S_{ls}$). See text for discussion.

Tests of the Susceptibility Model

Susceptibility to future failure by deep-seated sliding and earthflow, particularly estimates derived from old landslide deposits, is difficult to verify. ("Verify" probably is too strong a term. The extent to which earth-science predictions from a computer model can be evaluated, let alone validated, is a matter of much current debate; Oreskes, 2000.) Not only are the types of landslides addressed here less readily predicted than debris flows (statistical curves that relate rainfall intensity to its duration, of the sort cited by Haneberg, 2000, p. 214, do not exist for large, deep slides), but debris-flow prediction (Dietrich and others, 1993) is easier to test by virtue of being more DEM-dependent and based on landslide-occurrence data that are recent and frequent. (Also, similar triggering conditions can be assumed for all debris flows that occur in one storm.) Despite this comparative disadvantage and the limited data available, two evaluations were devised for the new susceptibility model, one outside the Project Impact area and one within.

We computed the susceptibility index for an adjacent area with similar geology, the Niles 7.5-minute quadrangle southeast of the Hayward quadrangle, and compared the results with the prevalence of old landslide deposits in that area (Nilsen, 1973b, 1975). S or S_{ls} was obtained for each 30-m cell in the Niles quadrangle, unit by geologic unit, by comparing the corresponding ground-slope value calculated from the Niles DEM with the appropriate slope:spatial frequency histogram (for example, fig. 6) derived in the Project Impact area. Figure 8A shows that the spatial frequency of 30-m cells coinciding with landslide deposits in the Niles quadrangle increases with the modeled susceptibility, from zero to 100 percent. The histogram maxima at values of 0.20-0.30 and 0.40-0.50 reflect steep slopes on the widespread and landslide-prone Briones Formation (Tbr). While this test is not wholly independent—the model is predicated on the correlation of high susceptibility with high spatial frequency of old landslide deposits (although in a different area than those in the test)—the positive correlation in figure 8A indicates that the model has identified potentially unstable terrain in the Niles quadrangle.

Table 4. Correspondence of recent landslide activity to modeled landslide susceptibility, showing the contrast between less hazardous and more hazardous geologic units

Modeled susceptibility for grid cells that contain 1,192 post-1970 landslides	Number of damaging post-1970 landslides		
	Undifferentiated by geologic unit	Differentiated by mean spatial frequency of old landslides on geologic units*	
		lower (< 0.10)	higher (>0.10)
0.00 - 0.09	514	438	76
0.10 - 0.19	180	68	112
0.20 - 0.29	112	10	102
0.30 - 0.39	147	0	147
0.40 - 0.49	149	1	148
0.50 - 1.20	90	0	90
	1,192	675	517

* from table 1

We also examined susceptibility estimates for the 1,192 post-1970 landslides—their 30-m grid cells were anticipated to be highly susceptible (defined provisionally here as values of S_{ls} and S >0.30). This expectation is not realized in the raw counts of the 1,192 recent failures, only 386 of which occur in cells where modeled susceptibility exceeds 0.30 (column 2 in table 4). Rather than indicating failure of the model, however, table 4 demonstrates the importance of anthropogenically influenced landsliding in Oakland, where human disturbance of the landscape has made formerly safe terrain hazardous.

To draw this distinction, we divided the 120 geologic units in table 1 into two groups, more hazardous and less hazardous, at 0.10, the median spatial frequency of old landslides. The resulting columns 3 and 4 of table 4 reveal a marked difference in the distribution of recent landslides with respect to the geologic units in which they occurred. Many of the 675 post-1970 slides in column 3 (in geologic units having a mean spatial frequency < 0.10) that are on grid cells with low modeled susceptibilities (0.00 - 0.29) are failures of graded cut-and-fill slopes in geologic units on flat-lying terrain in which pre-development failure was rare: alluvial fan (Qpaf, Qhaf, Qpoaf), the Garrity unit (Tcgl), and Novato Quarry terrane (Kfn). Few of these units (cited above) have modeled susceptibilities that exceed 0.30. In contrast, most of the 517 post-1970 landslides in column 4 of table 4 (in geologic units having a mean spatial frequency ≥0.10) occurred in the five hillside units known to be susceptible from their high frequency of old landslide deposits (also mentioned above): the Mulholland (Tmlu, Tmll) and Orinda (Tor) Formations, Franciscan Complex mélange (KJfm), and the large unnamed unit (Tus).

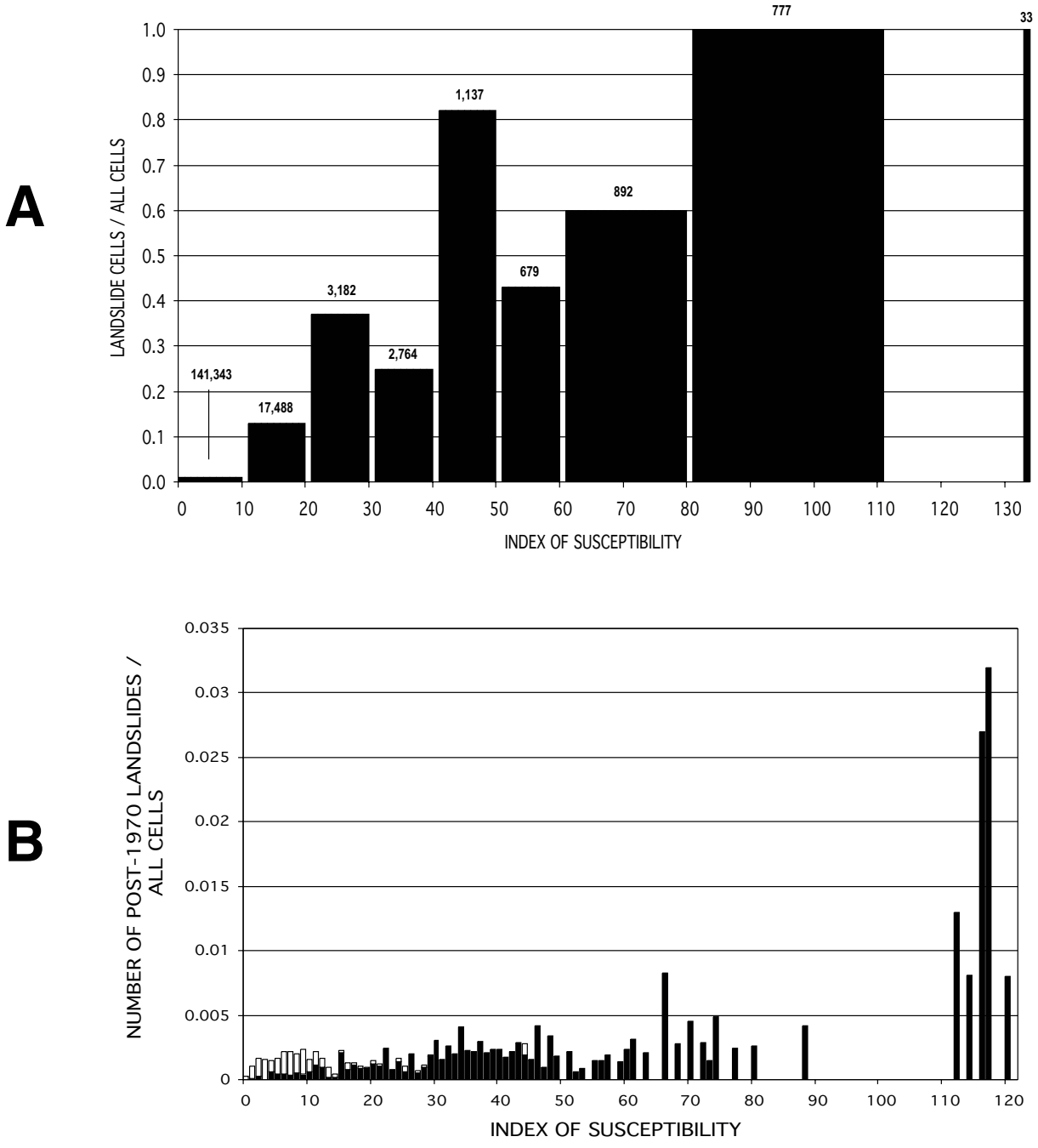

Figure 8. Histograms showing tests of the susceptibility model. A, Spatial frequency of old landslide deposits in the Niles quadrangle (SE of the Hayward quadrangle, fig. 1) as a function of modeled susceptibility; small numbers are grid-cell counts in each shaded bar. B, Spatial frequency of post-1970 damaging landslides in the study area, shown by number of slides (normalized by total grid cells with same index value) as a function of modeled susceptibility. For raw counts of post-1970 landslides see table 4. White portion of each bar: low-susceptibility geologic units; black portion: high-susceptibility units. See text for discussion.

Finally, the spatial frequency of the 1,192 post-1970 failures in figure 8B mimics the positive test results for the Niles quadrangle in figure 8A. The number of these recent landslides in figure 8B, normalized by the number of cells in each susceptibility interval, increases with values of the susceptibility index. Post-1970 landslides on low-hazard geologic units (white part of each histogram bar in figure 8B, according to the < 0.10 spatial-frequency criterion established above) are less prevalent with increasing model susceptibility, whereas recent failures on landslide-prone units (black parts of the bars, by the ≥0.10 spatial-frequency criterion) show the expected positive correlation.

The two evaluations suggest that our model or some variant of it, with due allowance for the destabilizing effects of grading in Quaternary deposits, can generate regional estimates of relative susceptibility, both within and outside the area in which the procedure was developed. In its present form the model is most applicable to bedrock formations in upland terrain. The model can be tested further as additional landslide inventories, such as those prepared recently by CDMG, become available in digital form. A robust test of the second type described here will require larger numbers of recent failures in different geologic units, as well as a sample unbiased toward damaging slides in developed terrain. The necessary data can come only from systematic mapping of all landslides regardless of their effects on the built environment. An alternative test might be designed to evaluate susceptibility modeling only for developed areas in Quaternary deposits. Table 5 summarizes some strengths and weaknesses of the current model and the map derived from it. Two of the shortcomings noted in table 5 reflect the data available for the Oakland area rather than the model itself.

Table 5. Summary evaluation of the susceptibility model and map

STRENGTHS	WEAKNESSES
Susceptibility is a continuous variable	Index number is relative only
Method is 100 percent quantitative	Some causative factors omitted
High resolution (that of DEM)	Requires large database
Spatial coverage is 100 %	Requires all-digital input
Can be applied to large areas	*Landslide inventory is not attributed or field-checked
Model is computationally transparent	*Slope data predate urbanization
Technique is exportable	

*the Oakland application only

THE SUSCEPTIBILITY MAP

The 969,003 values of susceptibility for all cells between (S) and within (S_{ls}) old landslide deposits (fig. 7D) are combined in one digital file and displayed on the map. The base information of topography, drainage, and culture is from an earlier 1:125,000-scale map (Aitken, 1997). Overall, our map resembles its sole predecessor, the 1:125,000-scale regional slope-stability map of Nilsen and Wright (1979), but differs greatly in detail. The map shows the continuous range of susceptibility, in decimal units, divided into eight intervals that broaden with increasing susceptibility and decreasing number of cells. The unequal intervals were chosen, after inspection of the frequency distribution (fig. 7D) and test plots (not shown), to emphasize the spatial variability of the index and yield a balanced-appearing map.

We have not assigned exact levels of landslide hazard to these susceptibility intervals, represented on the map by eight colors, other than an increasing susceptibility with warmth of tone and saturation of color, from gray to red. Which intervals to designate safe or dangerous is subjective and remains a matter of interpretation, as no direct means of calibration is available at this time. However, from field study that has long identified such geologic units as the Briones and Orinda Formations (Radbruch and Case, 1967; Radbruch, 1969; Keefer and Johnson, 1983; Bechini, 1993) as highly likely to fail (their mean spatial frequencies are 0.27-0.28, table 1), it appears that susceptibility values at least as low as 0.20 (yellow on the map) indicate areas of potential instability—depending on the strength and duration of triggering events. Dense clusters of values exceeding 0.30 (light orange on the map) are likely to contain areas of concern. Table 6 shows the distribution of the Project Impact area among the eight intervals, for the entire study area as well as its more susceptible hillside terrain (see table 3). We have not simplified the map into a few large "zones", convenient as these might be for regulatory applications. Because landsliding is a localized phenomenon, we find the concept of broad hazard zones unrealistic.

Table 6. Distribution of modeled susceptibility values on map

Index of Susceptibility	Percentage of map area: Entire area	Percentage of map area: Hillside geologic units only
< 0.01 (0)	37%	00 %
0.01-0.049	17	27
0.05-0.099	9	14
0.10-0.199	14	23
0.20-0.299	9	14
0.30-0.399	7	11
0.40-0.549	6	10
≥ 0.55	1	1

The map's spatial patterns are not random, but rather reveal a systematic relation between slope instability and contrasts in geology and the resulting NW-SE-trending topography, particularly the distribution of steep, high ridges. The susceptibility values that indicate the greatest potential hazard (>0.30) are conspicuous in steep terrain underlain by such geologic units as the lower member of the Mulholland Formation (Tmll), the Neroly Sandstone? (Tn?), the mudstone member of the Siesta Formation (Tst), an Eocene shale and claystone unit (Tshc), the widespread unnamed Tertiary sedimentary and volcanic unit (Tus), and also the Orinda (Tor) and Briones (Tbr) Formations. Table 6 shows that roughly 15 to 20 percent of the greater Oakland area is characterized by susceptibility values greater than 0.30. However, lower susceptibilities (in the 0.10-0.29 range) are common in Franciscan Complex mélange (KJfm) and other units known from field study (also evident by their high spatial frequencies in table 1) to be quite susceptible to sliding and earthflow. Some of the most susceptible localities in the map area are in the western Briones Valley quadrangle, the northern Oakland West quadrangle, the east-central Las Trampas Ridge quadrangle, and in the south-central Richmond quadrangle near the Hayward Fault. Most, but not all, locations on the map with the highest potential for slope failure are steep and thinly settled, commonly in parkland or areas unlikely to be developed.

A potential public-safety issue highlighted by this map is the location of residential dwellings in terrain likely to be unstable. Comparison of ABAG (1996) land-use data with this map (table 7) shows the percentage of residential housing in each of the eight levels of likely failure, for both the entire Project Impact area and the more susceptible hillsides within it (see table 3). Although most of the greater Oakland region lies within terrain having susceptibility-index values less than 0.05, 15 percent of the residential housing in hillside areas (covering nearly 20 km^2) is situated on terrain within the three highest levels of potential failure (≥0.30). One of the larger such convergences is located on the eastern slopes of Las Trampas Ridge in the town of Danville, west of San Ramon Creek. This residential area is underlain by an extensive landslide complex mapped by Nilsen that suggests highly susceptible rocks (unit Tn?; mean spatial frequency of old landslides in table 1 = 0.63) possibly related to the Neroly Sandstone (Tn)—the main body of which is much less susceptible (mean spatial frequency of old landslides in table 1 = 0.12). Hazard mapping by CDMG also ranked this area in its least-stable category (Majmundar, 1996b).

Table 7. Distribution of susceptibility values in land occupied by residential housing *

Index of Susceptibility	% Area in residential housing: Entire study area	% Area in residential housing: Hillside geologic units only
< 0.01 (0)	53%	00 %
0.01-0.049	20	43
0.05-0.099	7	15
0.10-0.199	8	17
0.20-0.299	4	9
0.30-0.399	4	9
0.40-0.549	3	5
≥ 0.55	1	1

* Land-use data from ABAG (1996)

APPLICATIONS AND LIMITATIONS

This map is a prototype for quantitative landslide-susceptibility coverage of the 10-county San Francisco Bay region. The digital geologic map (Wentworth, 1997) and slope data (Graham and Pike, 1998b) needed for this next step already exist, as well as some of the requisite landslide inventories (Pike, 1997) now available as digital-map files (Roberts and others, 1998, 1999). However, this map and similar products of GIS technology can aid in reducing the risk created by slope instability in the San Francisco Bay region only if they are used. It is the communication of susceptibility information to the public agencies and officials positioned to apply it, as well as guidance in its application, that ensures the success of such programs as Project Impact (Kockelman, 1979; Highland, 1997; Pike and others, 1998; Howell and others, 1999). The susceptibility model and map described here and projected research may be judged less by the quality or sophistication of the work than by whether their eventual use led to improved public safety or contributed to better land-use decisions (Olshansky and Rodgers, 1987; Mileti, 1999; Platt and others, 1999).

The information on this map is intended principally to assist public agencies in making planning decisions for the development or zoning of hillside locales within the greater Oakland area. Secondary uses include emergency preparedness through training exercises and dissemination of information on areas most likely to become unstable during an earthquake or after a season or succession of seasons of high rainfall. A successful example elsewhere in the San Francisco Bay area of the first application is the landslide-susceptibility map prepared by Brabb and others (1972) for San Mateo County. In 1973 and 1976, that County enacted ordinances that limited the density of development in geologically hazardous areas (defined as the three highest-susceptibility categories of the 1972 map) to as little as one dwelling unit per 16 hectares and required geologic reports and review by the County Geologist before any development was allowed. Over the last 25 years, these ordinances have been expanded in area and strengthened in their execution (Brabb, 1995). Kockelman (1979 and references therein) gives more examples of the application of USGS map products by public agencies in the San Francisco Bay region.

Because any prediction in the earth sciences is difficult at best (Oreskes, 2000) and hazard modeling is subject to great uncertainty (Haneberg, 2000), this map should be used with its limitations in mind. Most locations on the map that have high values of susceptibility are more likely to fail than locations with low values but almost certainly include areas that are not hazardous. More important from the viewpoint of public safety, most areas on the map showing low susceptibility are less prone to failure than areas of high values but are not without hazard. Some low susceptibility locales slope steeply and are subject to other types of failure. For example, landslide deposits less than 60 m in the longest dimension, which are common throughout the study area, were not included in the inventory on which this map is based. Many small failures may have resulted from debris flow, and the map does not depict that hazard. (Susceptibility to debris flow may be evaluated by computer methods differing from that devised here; Dietrich and others, 1993; Montgomery and Dietrich, 1994; Ellen and others, 1997; Campbell and others, 1998; Campbell and Chirico, 1999; Pack and others, 1999). Also, because landslide crowns and head scarps were not included in Nilsen's inventory and thus not incorporated into our model, terrain upslope of old deposits may be more susceptible than shown on this map. Finally, many deep-seated landslides simply cannot be predicted. Such failures result from chance blockage of surface drainage or other consequences of hillside development, as well as from the random operation of natural processes.

The caveats accompanying landslide inventories and susceptibility maps published by USGS and CDMG bear repeating (see also the comment on spatial resolution in the section, Digital Map Database, below). Geologic and climatic changes over the last few hundred thousand years have altered conditions of slope stability since initial movement of many (most?) of the observed landslide deposits in the Oakland area. Despite its 30-m level of detail our assessment is regional, based on a reconnaissance inventory that does not incorporate the composition or type of movement of individual landslide deposits. Our map estimates the relative importance of landsliding and, thus, overall stability, but it is only a guide to the likelihood of future movement. No frequency of failure per unit time is implied. In gauging the severity of slope instability, this map should be used together with local information on land use and soil and groundwater conditions.

Because detailed site investigations, under Chapters 7.5 and 7.8 of Division 2 of the California Public Resources Code, are required to judge the stability of a specific locale, this map is not a substitute for a report by a licensed engineering geologist or soils engineer (CDMG, 1997). This map does not carry the regulatory mandate of the official State of California landslide map (Wilson and others, 2000). Areas believed susceptible to landslide activity should be studied carefully before planning any development. In addition, surficial deposits other than landslides may pose construction problems and require a site investigation (Nilsen, 1973a, b; Nilsen and Wright, 1979). To gain a complete understanding of natural hazards, Oakland-area officials should consult maps that show susceptibility to debris flow, flooding, wildfire, earthquake ground-motion, soil liquefaction, and seismically induced slope failure (Haydon and others, 2000; Petersen and others, 2000).

FUTURE RESEARCH

Among advances embodied in this map are replacement of manual map-overlay by computer sorting, calculation of susceptibility as a continuous variable, high spatial resolution, narrow slope intervals, estimation of susceptibility within landslide deposits, and availability of the results as a digital file. Although we

doubt that the map can be quickly or easily improved upon as a quantitative first-order estimate of regional susceptibility to the kind of failures mapped by Nilsen (1975), the underlying model need not be static. Before basing further calculations on the model or extending its mapping beyond the Oakland area, it is prudent to weigh future courses of model development. Among these is consideration of variables that contribute to sliding and earthflow but are not included in the model (Brabb, 1995). To be practicable, additional data must be available over large areas, in digital-map format, and obtainable at modest effort and expense. Twelve candidate variables, mainly topographic parameters and generalized properties of geologic materials, are discussed briefly here. We have experimented with some of them.

(1) Ground-water level, a known trigger of deep landsliding, varies both seasonally and cyclically and thus is not strictly an attribute intrinsic to a site, but may be more appropriate to a model of landslide probability. Nonetheless, we did establish two general relations that may prove useful in incorporating this key variable into the susceptibility model. Mean annual precipitation (MAP) does not vary across the Oakland area in sufficient detail to provide a good proxy for ground-water level, but MAP does increase with (2) height above sea level (Rantz, 1971). Accordingly, we were not surprised to find that the spatial frequency of old landslide deposits in the Project Impact area also varies systematically with terrain elevation as expressed by the 30-m DEM (Graham and Pike, 1998a). The bell-shaped distribution of failure frequency with elevation (not shown) rises abruptly from 40 m to a maximum at about 210 m and tapers off above 600 m.

Because hillsides sheltered from afternoon sun commonly retain more moisture and thus may be more prone to instability than slopes facing the sun (Beaty, 1956), (3) slope exposure (aspect) in the lineated East Bay topography also can be expected to account for unexplained variance in our susceptibility model. However, the spatial scale most sensitive to differences in azimuth—probably a sub-grid larger than the usual default array of 3 × 3 cells—has yet to be identified. (4) Relative relief, vertical distance between highest and lowest elevations in an area (larger than that within which slope is customarily measured), also may supply useful information. While relief also may have an optimal spatial scale at which it influences landsliding, relief measured over a sample of any size rarely fails to correlate with slope (other than in such localized applications as the fine-scale transects measured by Schmidt and Montgomery, 1995) and thus could prove redundant.

(5) Slope curvature may be important in initiating failures other than debris flows, where it plays a critical role (Ellen and others, 1997; Dietrich and others, 1993; Pack and others, 1999). Convergent (concave upward and outward) hillslopes concentrate moisture (Richter, 1962; Beven, 1997) and thus may fail more readily than divergent (convex) or planar slopes, although exceptions to this generalization exist (Wójcik, 1997). Curvature is measured in profile and plan (Waltz, 1971; Evans, 1972), and has been modeled in both modes (Lanyon and Hall, 1983; Rowbotham and Dudycha, 1998; Irigaray and others, 1999). We experimented with profile curvature, the second derivative of elevation, calculating it for 30-m DEM cells from a 3 × 3 sub-grid. Averaged values of curvature for each of the 6,714 old slide masses neither usefully described the deposits nor provided contrasts in their frequency of occurrence that relate to susceptibility. The 3 × 3 sub-grid is too small to describe the relation of most mapped deposits to the gross curvature of surrounding topography, and testing is needed of sample designs that differ in size (and perhaps shape; Rowbotham and Dudycha, 1998).

A still-unexamined use of slope curvature that is likely to aid landslide prediction is the quantification of differences between frequency distributions pre- and post-failure. Accurate DEMs are required. While DEMs can be generated for landslide scarps and deposits from detailed surveys post-failure, pre-slide topography of comparable accuracy is unavailable. The usual sources of pre-slide DEMs in the Bay area and elsewhere, 1:24,000-scale contour maps, are unsatisfactory not only because of insufficient resolution and accuracy but also because they predate the landscape changes that resulted from hillside development in the 1950's and 1960's. High-resolution LIght Distance And Ranging (LIDAR) data acquired by airborne scanning pulsed-laser rangefinder are expected to eliminate this shortcoming (Ralph Haugerud, 2001, personal communication). Although currently expensive, LIDAR-generated DEMs soon will enable slope curvature and other terrain parameters to characterize landslide terrain with unprecedented accuracy.

Our unpublished tests on materials-properties data interpreted from Ellen and Wentworth (1995) show that (6) substrate expansivity correlates with landsliding, but this property is related to rock type and thus already is incorporated in the present model and map. While we found (7) bedding-dip direction (Radbruch and Weiler, 1963, table 2; Wentworth and others, 1987, p. 642) unrelated to landsliding in a sample of the study area, the convergence of bedding orientation with terrain slope (Schmidt and Montgomery, 1996 and references therein) warrants study in greater detail. Other site attributes remain unexamined. Among these are (8) bedding thickness and (9) fracture spacing (Ellen and Wentworth, 1995; Schmidt and Montgomery, 1996), (10) proximity to the Hayward Fault, and (11) vegetation type (now non-native in much of the study area).

The most effective additions to a model of regional susceptibility may not be natural site characteristics of Bay area hillsides. Because prediction of landsliding in areas of human habitation is of more immediate societal value than estimation of failure in unoccupied pristine terrain, the model needs parameters that better reflect susceptibility of slopes that have been modified to build residences and other structures. This enhancement of the model would diminish the number of low susceptibilities predicted for the obviously susceptible (by virtue of having failed) terrain in figure 8B. Natural physical controls on slope stability are unlikely to be among the candidate variables. The most promising alternative, we believe, is (12) horizontal distance to the nearest road, a parameter of proximity to disturbance of slopes by cut-and-fill grading—a major contributor to historic landsliding in the study area, particularly in units that are otherwise less susceptible (Nilsen and Turner, 1975, p. 6-7). The coincidence of recent damaging slides with suburban roads (fig. 3) supports this view.

Added factors will complicate or force abandonment of our susceptibility model, which is limited to three variables in its current implementation. Such changes are not to be undertaken lightly; prospective variables must demonstrate a significant contribution to susceptibility. The simplest approach to adding variables is to compute susceptibility for each variable as done here for ground slope and then combine the resulting values (weighted where appropriate) into a summary susceptibility. This method would preserve much of the original model's transparency.

Multivariate statistics (Cross, 1998; Brunori and others, 1996) is a more sophisticated method for adding landslide factors, but the explained variance thus gained must be weighed against losing the independent unit-by-unit determination of susceptibility, an important conceptual and computational advantage when analyzing large areas. Probit analysis, exemplified by the mapping of liquefaction susceptibility in the Monterey Bay area (Pike and others, 1994), is one multivariate technique that provides for such non-numerical (categorical) information as lithology, vegetation, and land use. Another multivariate technique adapted to landslide susceptibility (Massari and Atkinson, 1999), general linear modeling (Francis and others, 1993), also accommodates both numerical and non-numerical observations. Logistic regression, a third multivariate statistical tool, also has been applied to landsliding (Mark, 1992; Jäger and Wieczorek, 1994; Rowbotham and Dudycha, 1998).

Other questions warrant consideration in future development of the model. For example, estimates of susceptibility for old landslide deposits S_{ls} are based on the present slopes of those deposits, not the best values from which to predict movement because they describe topography that has already failed. Slope values better suited to model predictions would describe topography that has not yet failed, but will. Such measurements, obtainable only from surveyed profiles or DEMs of the same terrain both before and after failure has occurred, are unavailable for the study area and rare elsewhere (Yanagisawa and Umemura, 1999, p. 88). Recent experiments to find a temporary way around this problem (Pike and others, 1999a, b) suggest that a more refined model of susceptibility for sliding and earthflow might result from assumptions about (1) terrain geometry pre- and post-failure and (2) the coherence of earth materials on steep slopes. Implementing these assumptions would elevate susceptibility for the steeper terrain in existing landslide masses while not unduly raising or reducing it for the gentler terrain in those deposits:

> The overall frequency distribution of surface gradient in a landslide deposit, as expressed by mean slope, may be an acceptable starting-point from which to represent pre-slide topography. Two arguments favor this view. First, neither our experimental reconstructions of pre-slide terrain surrounding the landslide deposits nor our attempts to model the failure surface resulted in more credible values of susceptibility than use of the existing topography. Also, it has yet to be shown that pre- and post-slide frequency distributions of slope angle for the same piece of topography differ significantly—although the spatial distributions of those slopes obviously are not the same.
>
> Varied stability of the steepest slopes in an area of similar rock may reflect the contrasts in rock strength between and within existing landslide deposits. Steep slopes in the coherent bedrock between slides presumably are of low susceptibility because the physical properties of rock in undisturbed terrain (for example, continuous bedding and low density of fractures) resist failure. Low susceptibility should not be expected for steep slopes on landslide masses, however, where the disrupted, weakened rocks have different physical properties (discontinuous bedding, many fractures) and are likely to fail again. Accordingly, our model might be modified to allow susceptibility to reach its maximum values on the steepest terrain within old landslide deposits.

Finally, the model devised for the new map may contribute to more dynamic, scenario-based calculations. This map reveals the relative susceptibility of the greater Oakland area to sliding and earthflow, but not absolute susceptibility—that is, probability. A map of landslide probability requires coupling this map with historic information on the timing of precipitation amounts, groundwater levels, and landslide movements. Probability maps, in turn, can be combined with land-use data to create maps showing risk to the built environment. As a further step, data on economic valuation can be added to estimate the magnitude of possible future losses and conduct benefit-cost analyses for both proposed development and measures to mitigate the landslide hazard (Nilsen, Taylor and Brabb, 1976; Bernknopf and others, 1988). To fully appraise the slope-instability hazard in Oakland or any other area, such derivative maps would need to incorporate separate susceptibility calculations for debris flow, soil liquefaction, and earthquake-induced landsliding.

REFERENCES CITED

Aitken, D.S., 1997, A digital version of the 1970 U.S. Geological Survey topographic map of the San Francisco Bay region: U.S. Geological Survey Open-File Report 97-500, 3 map sheets, scale 1:125,000, [available on the World Wide Web at http://wrgis.wr.usgs.gov/open-file/of97-500].

Aniya, Masamu, 1985, Landslide-susceptibility mapping in the Amahata River basin, Japan: Annals of the Association of American Geographers, v. 75, no. 1, p. 102-114.

Association of Bay Area Governments (ABAG), 1996, Existing land use in 1995—data for Bay Area counties

and cities: Oakland, California, Association of Bay Area Governments [variously paged].

Atkinson, P.M., and Massari, Remo, 1998, Generalised linear modelling of susceptibility to landsliding in the central Apennines, Italy: Computers and Geosciences, v. 24, no. 4, p. 373-385.

Baum, R.L., Chleborad, A.F., and Schuster, R.L., 1998, Landslides triggered by the winter 1996-97 storms in the Puget Sound lowland, Washington: U.S. Geological Survey Open-File Report 98-239, 16 p., [available on the World Wide Web at http://geohazards.cr.usgs.gov/pubs/ofr/ofr98-239/ofr98-239.html].

Beaty, C.B., 1956, Landslides and slope exposure: Journal of Geology, v. 64, no. 1, p. 70-74.

Bechini, Claudia, 1993, Natural conditions controlling earth flows occurrence in the Eden Canyon area (San Francisco Bay region, California): Zeitschrift für Geomorphologie, Supplementband 87, p. 91-105.

Bernknopf, R.L., Campbell, R.H., Brookshire, D.S., and Shapiro, C.D., 1988, A probabilistic approach to landslide hazard mapping in Cincinnati, Ohio, with applications for economic evaluation: Bulletin of the Association of Engineering Geologists, v. 25, no. 1, p. 39-56.

Beven, K.J., 1997, TOPMODEL—a critique: Hydrological Processes, v. 11, no. 9, p. 1069-1085.

Bishop, C.C., Knox, R.D., Chapman, R.H., Rodgers, D.A., and Chase, G.B., 1973, Geological and geophysical investigations for Tri-Cities seismic safety and environmental resources study: California Division of Mines and Geology, Preliminary Report 19, 44 p., scale 1:24,000.

Blanc, R.P., and Cleveland, G.B., 1968, Natural slope stability as related to geology, San Clemente area, Orange and San Diego Counties, California: California Division of Mines and Geology, Special Report 98, 19 p., scale 1:20,000.

Brabb, E.E., 1995, The San Mateo County California GIS project for predicting the consequences of hazardous geologic processes, *in* Carrara, Alberto, and Guzzetti, Fausto, eds., International workshop, Geographical Information Systems in Assessing Natural Hazards, Perugia, Italy, September 20-22, 1993, Proceedings: Dordrecht, Kluwer, p. 299-334.

Brabb, E.E., and Pampeyan, E.H., 1972, Preliminary map of landslides in San Mateo County, California: U.S. Geological Survey Miscellaneous Field Studies Map MF-344, scale 1:62,500.

Brabb, E.E., Pampeyan, E.H., and Bonilla, M.G., 1972, Landslide susceptibility in San Mateo County, California: U.S. Geological Survey Miscellaneous Field Studies Map MF-360, scale 1:62,500.

Brunori, F., Casagli, N., Fiaschi, S., Garzonio, C.A., and Moretti, S., 1996, Landslide hazard mapping in Tuscany, Italy—an example of automatic evaluation, *in* Slaymaker, Olav, ed., Geomorphic Hazards: New York, Wiley, p. 56-67.

California Division of Mines and Geology (CDMG), 1997, Guidelines for evaluating seismic hazards in California: Sacramento, Department of Conservation, Special Publication 117, 74 p.

Campbell, R.H., Bernknopf, R.L., and Soller, D.R., 1998, Mapping time-dependent changes in soil slip-debris flow probability: U.S. Geological Survey Miscellaneous Investigations Series Map I-2586, 16 p. plus maps, scales 1:24,000 and 1:40,000.

Campbell, R.H., and Chirico, Peter, 1999, Geographic information system (GIS) procedure for preliminary delineation of debris-flow hazard areas from a digital terrain model, Madison County, Virginia: U.S. Geological Survey Open-File Report 99-336, 25 p.

Carrara, Alberto, Cardinali, Mauro, and Guzzetti, Fausto, 1992, Uncertainty in assessing landslide hazard and risk: ITC Journal, no. 1992-2, p. 172-183.

Carrara, Alberto, Cardinali, Mauro, Guzzetti, Fausto, and Reichenbach, Paola, 1995, GIS technology in mapping landslide hazard, *in* Carrara, Alberto, and Guzzetti, Fausto, eds., Geographical Information Systems in Assessing Natural Hazards, International workshop, Perugia, Italy, September 20-22, 1993, Proceedings: Dordrecht, Kluwer, p. 135-175.

Cleveland, G.B., 1971, Regional landslide prediction: Sacramento, California Division of Mines and Geology Open-File Report, 33 p.

Coe, J.A., Godt, J.W., Brien, Dianne, and Houdre, Nicolas, 1999, Map showing locations of damaging landslides in Alameda County, California, resulting from 1997-98 El Niño rainstorms: U.S. Geological Survey Miscellaneous Field Studies Map MF-2325-B, scale 1:125,000, [available on the World Wide Web at http://geology.cr.usgs.gov/pub/mf-maps/mf-2325-b/].

Cotton, W.R., and Cochrane, D.A., 1982, Love Creek landslide disaster January 5, 1982, Santa Cruz County: California Geology, v. 35, no. 7, p. 153-157.

Cross, Martin, 1998, Landslide susceptibility mapping using the matrix assessment approach—a Derbyshire case study, *in* Maund, J.G., and Eddleston, Malcolm, eds., Geohazards in engineering geology: London, Geological Society, Engineering Geology Special Publication 15, p. 247-261.

Dhakal, A.S., Amada, Takaaki, and Aniya, Masamu, 2000, Landslide hazard mapping and its evaluation using GIS—an investigation of sampling schemes for a grid-cell based quantitative method: Photogrammetric Engineering and Remote Sensing, v. 66, no. 8, p. 981-989.

Dietrich, W.E., Wilson, C.J., Montgomery, D.R., and McKean, James, 1993, Analysis of erosion thresholds, channel networks, and landscape morphology using a digital elevation model: Journal of Geology, v. 101, no.

2, p. 259-278, [available on the World Wide Web at http://socrates.berkeley.edu/~geomorph/shalstab/].

Ellen, S.D., 1988, Description and mechanics of soil slip/debris-flows in the storm, *in* Ellen, S.D., and Wieczorek, G.F., eds., Landslides, floods, and marine effects of the storm of January 3-5, 1982, in the San Francisco Bay Region, California: U.S. Geological Survey Professional Paper 1434, p. 63-112.

Ellen, S.D., and Wentworth, C.M., 1995, Hillside materials and slopes of the San Francisco Bay Region, California: U.S. Geological Survey Professional Paper 1357, 215 p., scale 1:125,000.

Ellen, S.D., Mark, R.K., Wieczorek, G.F., Wentworth, C.M., Ramsey, D.W., and May, T.E., 1997, Map showing principal debris-flow source areas in the San Francisco Bay region, California: U.S. Geological Survey Open-File Report 97-745 E, 8 p. plus maps, scale 1:125,000, [available on the World Wide Web at http://wrgis.wr.usgs.gov/open-file/of97-745/of97-745e.html].

Evans, I.S., 1972, General geomorphometry, derivatives of altitude and descriptive statistics, *in* Chorley, R.J., ed., Spatial analysis in geomorphology: New York, Harper and Row, p. 17-90.

Federal Emergency Management Agency (FEMA), 1998, Project Impact—building a disaster-resistant community: http://www.fema.gov/impact/.

Fernández, Tomás, Irigaray, Clemente, and Chacón, José, 1996, G.I.S. analysis and mapping of landslides determinant factors in the Contraviesa area (Granada, Southern Spain), *in* Chacón, José, Irigaray, Clemente, and Fernández, Tomás, eds., Landslides, International Conference and Field Trip, 8th, Granada, September 27-28, Proceedings: Rotterdam, Balkema, p. 141-151.

Francis, B., Green, M., and Payne, C., 1993, GLIM4—the statistical system for generalized linear interactive modeling: Oxford, Clarendon Press, 82 p.

Godt, J.W., ed., 1999, Maps showing locations of damaging landslides caused by El Niño rainstorms, winter season 1997-98, San Francisco Bay region, California: U.S. Geological Survey Miscellaneous Field Studies Map MF-2325-A-J, 12 p., scale 1:125,000, [available on the World Wide Web at http://geology.cr.usgs.gov/pub/mf-maps/mf-2325/]

Graham, S.E., and Pike, R.J., 1997, Shaded-relief map of the San Francisco Bay Region, California: U.S. Geological Survey Open-File Report 97-745 B, 8 p., scales 1:275,000 and 1:125,000, [available on the World Wide Web at http://wrgis.wr.usgs.gov/open-file/of97-745/of97-745b.html].

Graham, S.E., and Pike, R.J., 1998a, Elevation maps of the San Francisco Bay region, California; a digital database: U.S. Geological Survey Open-File Report 98-625, 17 p., scales 1:275,000 and 1:125,000, [available on the World Wide Web at http://wrgis.wr.usgs.gov/open-file/of98-625/index.html].

Graham, S.E., and Pike, R.J., 1998b, Slope maps of the San Francisco Bay region, California; a digital database: U.S. Geological Survey Open-File Report 98-766, 17 p., scales 1:275,000 and 1:125,000, [available on the World Wide Web at http://wrgis.wr.usgs.gov/open-file/of98-766/index.html].

Graymer, R.W., 2000, Geologic map and map database of the Oakland metropolitan area, Alameda, Contra Costa, and San Francisco Counties, California: U.S. Geological Survey Miscellaneous Field Studies Map MF-2342, 29 p., scale 1:50,000, [available on the World Wide Web at http://geopubs.wr.usgs.gov/map-mf/mf2342/].

Graymer, R.W., and Godt, J.W., 1999, Map showing locations of damaging landslides in Contra Costa County, California, resulting from 1997-98 El Niño rainstorms: U.S. Geological Survey Miscellaneous Field Studies Map MF-2325-E, one sheet, scale 1:125,000, [available on the World Wide Web at http://geology.cr.usgs.gov/pub/mf-maps/mf-2325-e/].

Haneberg, W.C., 2000, Deterministic and probabilistic approaches to geologic hazard assessment: Environmental and Engineering Geoscience, v. 6, no. 3, p. 209-226.

Haydon, W.D., 1995, Landslide hazards in the Martinez-Walnut Creek area, Contra Costa County, California: California Division of Mines and Geology Open-File Report 95-12, scale 1:24,000.

Haydon, W.D., Mattison, Elise, and Clahan, K.B., 2000, Liquefaction zones in the cities of Oakland and Piedmont, Alameda County, California, *in* Seismic hazard evaluation of the cities of Oakland and Piedmont, Alameda County, California: California Division of Mines and Geology Open-File Report 99-11, Section 1, p. 3-23, scale 1:24,000, [available on the World Wide Web at ftp://ftp.consrv.ca.gov/pub/dmg/shezp/evalrpt/OFR99-11.pdf].

Helley, E.J., and Graymer, R.W., 1997a, Quaternary geology of Alameda County, and parts of Contra Costa, Santa Clara, San Mateo, San Francisco, Stanislaus, and San Joaquin Counties, California—a digital database: U.S. Geological Survey Open-File Report 97-097, 8 p., [Available on the World Wide Web at http://wrgis.wr.usgs.gov/open-file/of97-97/].

Helley, E.J., and Graymer, R.W., 1997b, Quaternary geology of Contra Costa County, and surrounding parts of Alameda, Marin, Sonoma, Solano, Sacramento, and San Joaquin Counties, California—a digital database: U.S. Geological Survey Open-File Report 97-098, 8 p., [Available on the World Wide Web at http://wrgis.wr.usgs.gov/open-file/of97-98/].

Highland, L.M., 1997, Landslide hazard and risk—current and future directions for the United States Geological Survey's landslide program, *in* Cruden, D.M., and Fell, Robin, eds., Landslide risk assessment: Rotterdam, Balkema, p. 207-213.

Howell, D.G., Brabb, E.E., and Ramsey, D.W., 1999, How useful is landslide hazard information? Lessons learned in the San Francisco Bay region: International Geology Review, v. 41, no. 4, p. 368-381.

Hylland, M.D., and Lowe, Mike, 1997, Regional landslide-hazard evaluation using landslide slopes, western Wasatch County, Utah: Environmental Engineering and Geoscience, v. 3, no. 1, p. 31-43.

Irigaray Fernández, Clemente, Fernández del Castillo, Tomás, El Hamdouni, Rachid, and Chacón Montero, José, 1999, Verification of landslide susceptibility mapping—a case study: Earth Surface Processes and Landforms, v. 24, no. 6, p. 537-544.

Jäger, Stefan, and Wieczorek, G.F., 1994, Landslide susceptibility in the Tully Valley area, Finger Lakes region, New York: U.S. Geological Survey Open-File Report 94-615, scale 1:24,000.

Jayko, A.S., Rymer, M.J., Prentice, C.S., Wilson, R.C., and Wells, R.E., 1998, The Scenic Drive Landslide Jan.-Feb. 1998, La Honda, San Mateo County, California: U.S. Geological Survey Open-File Report 98-229, one plate.

Jennings, P.J., and Siddle, H.J., 1998, Use of landslide inventory data to define the spatial location of landslide sites, South Wales, United Kingdom, *in* Maund, J.G., and Eddleston, Malcolm, eds., Geohazards in engineering geology: London, Geological Society, Engineering Geology Special Publication 15, p. 199-211.

Jones, F.O., Embody, D.R., and Peterson, W.L., 1961, Landslides along the Columbia River valley, northeastern Washington: U.S. Geological Survey Professional Paper 367, 98 p.

Keefer, D.K., Griggs, G.B., and Harp, E.L., 1998, Large landslides near the San Andreas fault in the Summit Ridge area, Santa Cruz Mountains, California, *in* Keefer, D.K., ed., The Loma Prieta, California, Earthquake of October 17, 1989—Landslides: U.S. Geological Survey Professional Paper 1551-C, p. C71-C128.

Keefer, D.K., and Johnson, A.M., 1983, Earth flows—morphology, mobilization, and movement: U.S. Geological Survey Professional Paper 1264, 56 p.

Kockelman, W.J., 1979, The use of U.S. Geological Survey earth-science products by selected regional agencies in the San Francisco Bay region, California: U.S. Geological Survey Open-File Report 79-221, 173 p.

Lanyon, L.E., and Hall, G.F., 1983, Land-surface morphology; 2, predicting potential landscape instability in eastern Ohio: Soil Science, v. 136, no. 6, p. 382-386.

Liang, Ta, and Belcher, D.J., 1958, Airphoto interpretation, chap. 5 *of* Eckel, E.D., ed., Landslides and engineering practice: Wash., D.C., Highway Research Board, National Research Council Special Report 29, p. 69-92.

Majmundar, H.H., 1996a, Landslide hazards in the Hayward quadrangle and parts of the Dublin quadrangle, Alameda and Contra Costa Counties, California: California Division of Mines and Geology Open-File Report 95-14, scale 1:24,000.

Majmundar, H.H., 1996b, Landslide hazards in the Las Trampas Ridge quadrangle and parts of the Diablo quadrangle, Alameda and Contra Costa Counties, California: California Division of Mines and Geology Open-File Report 95-15, scale 1:24,000.

Mark, R.K., 1992, Map of debris-flow probability, San Mateo County, California: U.S. Geological Survey Miscellaneous Investigations Series Map I-1257-M, 2 sheets, scale 1:62,500.

Massari, Remo, and Atkinson, P.M., 1999, Modeling susceptibility to landsliding—an approach based on individual landslide type: Transactions, Japanese Geomorphological Union, v. 20, no. 3, p. 151-168.

McHarg, I.L., 1969, Design with nature: Garden City, The Natural History Press, 198 p.

Miles, S.B., and Keefer, D.K., 2000, Evaluation of seismic slope-performance models using a regional case study: Environmental and Engineering Geoscience, v. 6, no. 1, p. 25-39.

Mileti, Dennis, 1999, Disasters by design—a reassessment of natural hazards in the United States: Washington, D.C., Joseph Henry Press, 376 p.

Miller, D.J., 1995, Coupling GIS with physical models to assess deep-seated landslide hazards: Environmental and Engineering Geoscience, v. 1, no. 3, p. 263-276.

Montgomery, D.R., and Dietrich, W.E., 1994, A physically based model for the topographic control on shallow landsliding: Water Resources Research, v. 30, no. 4, p. 1153-1171, [available on the World wide Web at http://socrates.berkeley.edu/~geomorph/shalstab/].

Mora, Sergio, and Vahrson, W.-G., 1994, Macrozonation methodology for landslide hazard determination: Bulletin of the Association of Engineering Geologists, v. 31, no. 1, p. 49-58.

Neuland, Herbert, 1976, A prediction model of landslips: Catena, v. 3, no. 2, p. 215-230.

Newman, E.B., Paradis, A.R., and Brabb, E.E., 1977, Feasibility and cost of using a computer to prepare landslide susceptibility maps of the San Francisco Bay region, California: U.S. Geological Survey Bulletin 1443, 27 p.

Nilsen, T.H., 1973a, Preliminary photointerpretation map of landslide and other surficial deposits of the Concord 15-minute quadrangle and the Oakland West, Richmond, and part of the San Quentin 7.5-minute quadrangles, Contra Costa and Alameda Counties, California: U.S. Geological Survey Miscellaneous Field Studies Map MF-493, scale 1:62,500.

Nilsen, T.H., 1973b, Preliminary photointerpretation map of landslide and other surficial deposits of the Livermore and parts of the Hayward 15-minute quadrangles, Alameda and Contra Costa Counties, California: U.S. Geological Survey Miscellaneous Field Studies Map MF-519, scale 1:62,500.

Nilsen, T.H., 1975, Preliminary photo-interpretation maps of landslide and other surficial deposits of 56 7.5-minute quadrangles, Alameda, Contra Costa, and Santa Clara Counties, California (with parts of adjoining counties on several maps by John A. Bartow, Virgil A. Frizzell, Jr., and John D. Sims): U.S. Geological Survey Open-File Report 75-277, scale 1:24,000.

Nilsen, T.H., Taylor, F.A., and Brabb, E.E., 1976, Recent landslides in Alameda County, California (1940-71)—an estimate of economic losses and correlations with slope, rainfall, and ancient landslide deposits: U.S. Geological Survey Bulletin 1398, 21 p., scale 1:62,500.

Nilsen, T.H., Taylor, F.A., and Dean, R.M., 1976, Natural conditions that control landsliding in the San Francisco Bay region—an analysis based on data from the 1968-69 and 1972-73 rainy seasons: U.S. Geological Survey Bulletin 1424, 35 p., scale 1:250,000.

Nilsen, T.H., and Turner, B.L., 1975, Influence of rainfall and ancient landslide deposits on recent landslides (1950-71) in urban areas of Contra Costa County, California: U.S. Geological Survey Bulletin 1388, 18 p.

Nilsen, T.H., and Wright, R.H., 1979, Relative slope stability of the San Francisco Bay region, *in* Nilsen, T.H., Wright, R.H., Vlasic, T.C., and Spangle, W.E., Relative slope stability and land-use planning in the San Francisco Bay region, California: U.S. Geological Survey Professional Paper 944, p. 16-55, scale 1:125,000.

Olshansky, R.B., and Rogers, J.D., 1987, Unstable ground—landslide policy in the United States: Ecological Law Quarterly, v. 13, no. 4, p. 939-1006.

Oreskes, Naomi, 2000, Why predict? Historical perspectives on prediction in the earth sciences, *in* Sarewitz, Daniel, Pielke, R.A. Jr., and Byerly, Radford Jr., eds., Prediction—science, decision making, and the future of nature: Washington, D.C., Island Press, p. 23-40.

Pachauri, A.K., and Pant, Manoj, 1992, Landslide hazard mapping based on geological attributes: Engineering Geology, v. 32, no. 12, p. 81-100.

Pack, R.T., Tarboton, D.G., and Goodwin, C.N., 1999, GIS-based landslide susceptibility mapping with SINMAP, *in* Bay, J.A., ed., Symposium on engineering geology and geotechnical engineering 34th, Logan, Utah, April 28-30, 1999, Proceedings: Pocatello, Idaho State University, p. 219-231.

Petersen, M.D., Cramer, C.H., Faneros, G.A., Real, C.R. and Reichle, M.S, 2000, Potential ground shaking in the cities of Oakland and Piedmont, Alameda County, California, *in* Seismic hazard evaluation of the cities of Oakland and Piedmont, Alameda County, California: California Division of Mines and Geology Open-File Report 99-11, Section 3, p. 55-64, scale 1:24,000, [available on the World Wide Web at ftp://ftp.consrv.ca.gov/pub/dmg/shezp/evalrpt/OFR99-11.pdf].

Pike, R.J., 1988, The geometric signature—quantifying landslide-terrain types from digital elevation models: Mathematical Geology, v. 20, no. 5, p. 491-511.

Pike, R.J., 1997, Index to detailed maps of landslides in the San Francisco Bay region, California: U.S. Geological Survey Open-File Report 97-745 D, 20 p. and map, [available on the World Wide Web at http://wrgis.wr.usgs.gov/open-file/of97-745/of97-745d.html].

Pike, R.J., Bernknopf, R.L., Tinsley, J.T., III, and Mark, R.K., 1994, Hazard of earthquake-induced lateral-spread ground failure on the central California coast modeled from earth-science map data in a geographic information system: U.S. Geological Survey Open-File Report 94-662, 46 p.

Pike, R.J., Graymer, R.W., and Roberts, Sebastian, 1999a, GIS-based mapping of landslide susceptibility in the San Francisco Bay area, California [abs.]: Geological Society of America Abstracts with Programs, v. 31, no. 7, p. A-195.

Pike, R.J., Graymer, R.W., and Roberts, Sebastian, 1999b, Regional modeling of landslide susceptibility in the San Francisco Bay region, California [abs.]: Eos Transactions of the American Geophysical Union, v. 80, no. 46 (Supplement), p. F450.

Pike, R.J., Cannon, S.H., Ellen, S.D., Graham, S.E., and others, 1998, Slope failure and shoreline retreat during northern California's latest El Niño: GSA Today, v. 8, no. 8, p. 1-6.

Platt, R.H., ed., with O'Donnell, K.B., and Scherf, David, contributors, 1999, Disasters and democracy—the politics of extreme natural events: Washington, D.C., Island Press, 335 p.

Radbruch, D.H., 1969, Areal and engineering geology of the Oakland East quadrangle, California: U.S. Geological Survey Geologic Quadrangle Map GQ-769, scale 1:24,000.

Radbruch, D.H., 1970, Map showing areas of relative amounts of landslides in California: U.S. Geological Survey Open-File Report 70-270, 36 p., scale 1:500,000.

Radbruch, D.H., and Case, J.E., 1967, Preliminary geologic map and engineering geologic information, Oakland and vicinity, California: U.S. Geological Survey, Open-File Report 67-183, 2 sheets, scale 1:24,000.

Radbruch, D.H., and Weiler, L.M., 1963, Preliminary report on landslides in a part of the Orinda Formation, Contra Costa County, California: U.S. Geological

Survey Open-File Report 689, 35 p., 14 pp. of tables, scale 1:24,000.

Rantz, S.E., 1971, Iso-hyetal map of San Francisco Bay Region, California, showing mean annual precipitation and precipitation depth-duration-frequency data: San Francisco Bay Region Environmental and Resources Planning Study Basic Data Contribution 25, 23 p., scale 1:500,000.

Reneau, S.L., Dietrich, W.E., Dorn,R.I., Berger, C.R., and Rubin, Meyer, 1986, Geomorphic and paleoclimate implications of latest Pleistocene radiocarbon dates from colluvium-mantled hollows, California: Geology, v. 14, no. 8, p. 655-658.

Richter, Hans, 1962, Eine neue Methode der großmaßstäblichen Kartierung des Reliefs [a new method of large-scale relief mapping]: Petermanns Geographische Mitteilungen, v. 106, no. 4, p. 309-312.

Ritchie, A.M., 1958, Recognition and identification of landslides, chap. 4 *of* Eckel, E.D., ed., Landslides and engineering practice: Wash., D.C., Highway Research Board, National Research Council, Special Report 29, p. 48-68.

Roberts, Sebastian, Barron, Andrew, Brabb, E.E., and Pike, R.J., 1998, Digital compilation of "Preliminary map of landslide deposits in Santa Cruz County, California, by Cooper-Clark and Associates, 1975"—a digital map database: U.S. Geological Survey Open-File Report 98-792, 22 p., [available on the World Wide Web at http://wrgis.wr.usgs.gov/open-file/of98-792].

Roberts, Sebastian, Roberts, M.A., Brennan, E.M., and Pike, R.J., 1999, Landslides in Alameda County, California, a digital database extracted from Preliminary Photointerpretation Maps of Surficial Deposits by T.H. Nilsen in USGS Open-File Report 75-277: U.S. Geological Survey Open-File Report 99-504, 20 p., [available on the World Wide Web at http://wrgis.wr.usgs.gov/open-file/of99-504/].

Rogers, T.H., and Armstrong, C.F., 1971, Environmental geologic analysis of the Santa Cruz Mountains study area, Santa Clara County, California: California Division of Mines and Geology, Open-File Report 72-21, 101 p., scale 1:12,000.

Roth, R.A., 1983, Factors affecting landslide-susceptibility in San Mateo County, California: Bulletin of the Association of Engineering Geologists, v. 20, no. 4, p. 353-372.

Rowbotham, D.N., and Dudycha, Douglas, 1998, GIS modelling of slope stability in Phewa Tal watershed, Nepal: Geomorphology, v. 26, nos. 1-3, p. 151-170.

Schmidt, K.M., and Montgomery, D.R., 1995, Limits to relief: Science, v. 270, no. 5236, p. 617-620.

Schmidt, K.M., and Montgomery, D.R., 1996, Rock mass strength assessment for bedrock landsliding: Environmental and Engineering Geoscience, v. 2, no. 3, p. 325-338.

Soeters, Robert, and van Westen, C.J., 1996, Slope instability recognition, analysis, and zonation *in* Turner, K.A., and Schuster, R.L., eds., Landslides, investigation and mitigation: Wash., D.C., Transportation Research Board, National Research Council, Special Report 247, p. 129-177.

Stromberg, P.A., 1967, Landslide problems related to housing development in central California: San Francisco, San Francisco State College, unpublished M.A. thesis, 137 p.

Turrini, M.C., and Visintainer, Paola, 1998, Proposal of a method to define areas of landslide hazard and application to an area of the Dolomites, Italy: Engineering Geology, v. 50, nos. 3-4, p. 255-265.

U.S. Geological Survey, 1993, Digital elevation models—data users guide 5: Reston, Va., U.S. Geological Survey, 48 p.

Van Horn, Richard, 1972, Relative slope stability map of the Sugar House quadrangle, Salt Lake County, Utah: U.S. Geological Survey Miscellaneous Investigations Series Map I-766-E, 1:24,000 scale.

Van Westen, C.J., Rengers, N., Terlien, M.T.J., and Soeters, R., 1997, Prediction of the occurrence of slope instability phenomena through GIS-based hazard zonation: Geologische Rundschau, v. 86, no. 2, p. 404-414.

Varnes, D.J., 1978, Slope movement and types and processes, chap. 2 *of* Schuster, R.L., and Krizek, R.J., eds., Landslides: analysis and control: Wash., D.C., Transportation Research Board, National Academy of Sciences, Special Report 176, p. 11-33.

Wagner, J.R., 1978, Late Cenozoic history of the Coast Ranges east of San Francisco Bay: Berkeley, University of California, Ph.D. dissertation, 160 p., 12 pls.

Waltz, J.P., 1971, An analysis of selected landslides in Alameda and Contra Costa Counties, California: Bulletin of the Association of Engineering Geologists, v. 8, no. 2, p. 153-163.

Wentworth, C.M., 1997, General distribution of geologic materials in the San Francisco Bay region, California, 1:125,000 scale—a digital map database: U.S. Geological Survey Open-File Report 97-744, 24 p., [available on the World Wide Web at http://wrgis.wr.usgs.gov/open-file/of97-744].

Wentworth, C.M., Ellen, S.D., and Mark, R.K., 1987, Improved analyses of regional engineering geology using geographic information systems, *in* GIS-San Francisco, International Conference, Exhibits, and Workshops on Geographic Information Systems, 2nd, San Francisco, October 26-30, 1987, Proceedings: American Society for Photogrammetry and Remote Sensing/American Congress on Surveying and Mapping, v. 2, p. 636-649.

Wentworth, C.M., Graham, S.E., Pike, R.J., Beukelman, G.S., Ramsey, D.W., and Barron, A.D., 1997, Summary

distribution of slides and earth flows in the San Francisco Bay region, California: U.S. Geological Survey Open-File Report 97-745 C, 10 p., 11 sheets, [available on the World Wide Web at http://wrgis.wr.usgs.gov/open-file/of97-745/of97-745c.html].

Wieczorek, G.F., 1984, Preparing a detailed landslide-inventory map for hazard evaluation and reduction: Bulletin of the Association of Engineering Geologists, v. 21, no. 3, p. 337-342.

Wills, C.J., and Majmundar, H.H., 2000, Landslide hazard Map of southwest Napa County, California: California Division of Mines and Geology, Open-File Report 99-06, scale 1:24,000.

Wilson, R.I., McCrink, T.P., McMillan, J.R., and Haydon, W.D., 2000, Earthquake-induced landslide zones in the cities of Oakland and Piedmont, Alameda County, California, *in* Seismic hazard evaluation of the cities of Oakland and Piedmont, Alameda County, California: California Division of Mines and Geology Open-File Report 99-11, Section 2, p. 35-54. scale 1:24,000, [available on the World Wide Web at ftp://ftp.consrv.ca.gov/pub/dmg/shezp/evalrpt/OFR99-11.pdf].

Wilson, R.C., and Jayko, A.S., 1997, Preliminary maps showing rainfall thresholds for debris-flow activity, San Francisco Bay region, California: U.S. Geological Survey Open-File Report 97-745 F, 20 p., 2 sheets, scale 1:275,000, [available on the World Wide Web at http://wrgis.wr.usgs.gov/open-file/of97-745/of97-745f.html].

Wójcik, Antoni, 1997, Landslides in the Koszarawa drainage basin—structural and geomorphological control (western Carpathians, Beskid Zywiecki Mts.): Biuletyn Panstwowego Instytutu Geologicznego, no. 376, p. 31-42.

Yanagisawa, Eiji, and Umemura, Jun, 1999, Geotechnical features of the Hachimantai-Sumikawa landslide: Journal of Natural Disaster Science, v. 20, no. 2, p. 83-92.

APPENDIX — THE DIGITAL MAP DATABASE

INTRODUCTION

This report provides digital data and plottable files that depict the relative susceptibility to certain types of slope failure in the Oakland area, California, at 30-m ground resolution. Although the susceptibility calculations described in the body of the report were derived from digital maps of geology, terrain slope, and landslides, only data for the susceptibility map are included here.

The input data on geology, slope, and landslides were compiled and the susceptibility calculations performed in ARC/INFO, a commercial geographic information system (GIS) (Environmental Research Institute [ESRI], Redlands, California), by a program written in Arc Macro Language (AML) for the GRID extension of ARC/INFO.

The resulting landslide-susceptibility database consists of a data layer called susgrd_utm, described in table 1 below. The map layer is stored in UTM projection (zone 10; see table 2); projection files are included to convert between UTM and the state plane projection. Digital tics define a 7.5-minute grid of latitude and longitude. Contents of the map database are described as susceptibility values in 30-m grid cells. Terms in table 3 describe the database fields.

Table 1. Data layers

Data layer name	Description
susgrd_utm	30-meter raster grid containing the susceptibility values
drain	Vector coverage of drainage base
culture	Vector coverage of cultural base
roads	Vector coverage of road network base
hwys	Vector coverage of interstate highway base
hydro	Vector coverage of hydrological base

Table 2. Map projection

Projection	UTM (universal transverse mercator)
Units	meters
Zone	10
Datum	NAD 27
Spheroid	Clark 1886

Table 3. Field definition terms

ITEM NAME	Name of database field (item)
WIDTH	Maximum number of digits or characters stored
OUTPUT	Output width
TYPE	B - binary integer, F - binary floating point number, N - ASCII floating point number, I - ASCII integer, C - ASCII character string
N.DEC	Number of decimal places maintained for floating point numbers

Susceptibility values are stored for individual 30-meter grid cells, and are tabulated in the 'count' column (see table 4).

Table 4. Content of the value attribute table (SUSGRD_UTM.PAT)

Item name	Width	Output	Type	N.DEC	Description
VALUE	4	10	B	--	Susceptibility value
COUNT	4	10	B	--	Number of cells with corresponding value

The susceptibility values in table 4 are distributed in the 1:50,000-scale map, which contains 1112 rows and 1394 columns. The number of different susceptibility values is 110; the minimum value is 0.0, the maximum 133.0, the mean 13.2, and the standard deviation 18.1. Because the distribution of susceptibility values is highly skewed (see text figure 7D), the latter two statistics are given for reference only.

SPATIAL RESOLUTION

Uses of this digital map should not violate the spatial resolution of the data. Although the digital form of the data removes the physical constraint imposed by the scale of a paper map, the detail and accuracy inherent in map scale are also present in the digital data. Because this database was extracted from maps at a scale of 1:24,000 and compiled at that same scale, higher-resolution information is not present. Enlargement of the database to scales larger than 1:24,000 will not yield greater real detail, although it may reveal fine-scale irregularities below the intended resolution of the database. Similarly, where this database is used in combination with other data of higher resolution, the resolution of the combined output will be limited by the lower resolution of these data.

OVERVIEW OF THE DIGITAL DATABASE

This report consists of a 1:24,000-scale digital database, a 1:50,000-scale digital map image derived from it entitled "Map and Map Database of Susceptibility to Slope Failure by Sliding and Earthflow in the Oakland Area, California," and supporting files. The report is stored as several digital files: the spatial data as both ARC export (uncompressed) and ARCVIEW shape formats, and the map image as both Postscript and PDF formats. The exported

ARC coverages lie in UTM zone 10 projection and the shape versions are coded in decimal degrees. This pamphlet, which fully describes preparation of the digital map database as well as its content and character, is included as Postscript, PDF, and ASCII text files and is also available on paper as USGS Miscellaneous Field Studies Map MF-2385.

A plotted copy of the 1:50,000-scale map can be ordered from a USGS Earth Science Information Center or by telephone at 1-888-ASK-USGS. Any or all of the digital files can be obtained over the Internet or by magnetic tape copy, as described at the end of this section. The full versatility of the 1:24,000-scale spatial database is realized by importing the ARC export files into ARC/INFO or an equivalent GIS. Other GIS packages, including MapInfo and ARCVIEW, can use either the ARC export or shape files. The Postscript map image can be used for viewing or plotting in computer systems with sufficient capacity, and the considerably smaller PDF image files can be viewed or plotted in full or in part from Adobe ACROBAT software running on Macintosh, PC, or UNIX platforms.

DATABASE CONTENTS

The six sets of digital files comprising the database are encoded in more than one format. Names of the files are unique designators based on the report identifier, MF-2385, followed by part numbers (1 through 6 below) and an extension indicating file type. Some files have been bundled using the tar (UNIX Tape Archive) utility (.tar extension). All larger files have been compressed with the gzip utility, indicated by the .gz extension. The files and their identities are as follows:

1. Revision list: A list of the parts of the report and at what version number of the report each was last revised (if at all) followed by a chronological list that describes any revisions (see REVISIONS, below).

MF-2385revs_1a.txt	ASCII file

2. Text: The pamphlet (this text), which describes the database and how to obtain it.

MF-2385_2a.txt	ASCII file
MF-2385_2b.ps	Postscript file
MF-2385_2c.pdf	PDF file

3. Database of susceptibility values: ARC GRID containing 30-meter cells. Import.aml will name this grid susgrd_utm.

MF-2385_3.e00.gz	Arc export grid

4. Supporting files for ARC/INFO use, bundled as one tar file: When opened, the tar file yields:

sp2utm.prj

and

utm2sp.prj

which are projection files to convert between the UTM zone 10 projection of the database and state plane projection,

and

import.aml:

which is an ASCII script written in Arc Macro Language for converting the ARC export files into usable coverages and INFO files that are assigned standard names (see IMPORTING THE ARC EXPORT FILES).

5. Quadrangle index database: The data files representing lines and polygons of the quadrangle index (ARC export and ARCVIEW shape format). The ARC version also includes quadrangle names as annotation.

MF-2385_5a.e00.gz MF-2385_5b.e00.gz MF-2385_5c.e00.gz MF-2385_5d.e00.gz MF-2385_5e.e00.gz	ARC export files containing lines, polygons, and annotation.
MF-2385_5.tar.gz	Line and polygon ARCVIEW shape files bundled as one tar file. When opened, the tar file yields:

Polygon files:

MF-2385_5a.dbf	MF-2385_5a.shp	MF-2385_5a.shx
MF-2385_5b.dbf	MF-2385_5b.shp	MF-2385_5b.shx
MF-2385_5c.dbf	MF-2385_5c.shp	MF-2385_5c.shx
MF-2385_5d.dbf	MF-2385_5d.shp	MF-2385_5d.shx
MF-2385_5e.dbf	MF-2385_5e.shp	MF-2385_5e.shx

6. Plot files for the map: "Map and Map Database of Susceptibility to Slope Failure by Sliding and Earthflow in the Oakland Area, California," which measures 30 by 51 inches when plotted.

MF-2385_6a.eps	Postscript file (39.6 MB)
MF-2385_6b.pdf	PDF file (13 MB) Available on Adobe Acrobat Version 4.0

REVISIONS

Any part of the report (the numbered items described above and listed in the revision list MF-2385revs_a.txt) may be changed in the future if needed. Changes could involve, for example, fixing files that don't work, correcting or adding landslide, geology, or slope details, or adding new file formats or other components. Any major revision to the input data or the susceptibility model would result in a new report.

The report begins at version 1.00. Any revisions will be noted in the revision list and will result in the recording of a new version number for the report. Small changes will be indicated by decimal increments and larger changes by integer increments in the version number. Revisions will be announced and maintained on the Web page for this report on the Western Region geologic publications server (see next section).

OBTAINING THE DATABASE FILES

The database may be obtained in three ways.

1. The simplest is to download it over the World Wide Web from the USGS Western Region geologic publications server:

http://geopubs.wr.usgs.gov

You also can go directly to:

http://wrgis.wr.usgs.gov/map-mf/mf2385/

On this page, the several parts of the report in their different file types are available separately. Set your Web browser to save to a local disk and click on the appropriate links to download the desired files.

2. To download the files from the Internet via anonymous ftp:

ftp wrgis.wr.usgs.gov	- make ftp connection with USGS computer wrgis
Name: anonymous	- enter "anonymous" as your user name.
Password: [your address]	- enter your own email address as password.
pub/???/MF-2385	- subdirectory where files from this report are stored

3. To obtain files from the database on compact disc (CD), send a blank CD with your request specifying the desired files and your return address to:

Oakland Slope Failure Susceptibility Map Database
c/o Database Coordinator
U.S. Geological Survey
345 Middlefield Road MS 975
Menlo Park, CA 94025

The specified files bundled in a compressed tar file will be returned to you on the disc. The acceptable disc types are: CD-R or CD-RW discs.

OPENING THE DATABASE FILES

Some of the files are packaged as tar files, and the larger files containing the databases and images have been compressed with gzip. Thus, gzip is required to uncompress the files, and a tar utility is required to open the tar files. The necessary utilities are available on-line:

Compressed Gzip Files

Files compressed with gzip (those with a .gz extension) can be uncompressed with gzip. The gzip utility converts the compressed file name.gz to its uncompressed equivalent name. The compressed file is replaced by the uncompressed file. This utility is free of charge over the Internet at:

http://www.gzip.org/

Tar Files (UNIX Tape Archive)

To extract the contents of a tar file, first uncompress it with gzip if the extension is .tar.gz. Once the tar extension is exposed, extract the contents with a tar utility. This utility is included in most UNIX systems. Tar utilities for PC and Macintosh can be obtained free of charge via the Internet from Internet Literacy's Common Internet File Formats Web Page:

http://www.matisse.net/files/formats.html

WinZip

This commercial package runs on PCs and can deal with both gzip and tar files. An evaluation copy of WinZip for Windows 3.1, 95 and NT can be downloaded from:

http://www.winzip.com/winzip/

IMPORTING THE ARC EXPORT FILES

(Note that the export files are ASCII files. Hold down the shift key when you click to download)

The ARC export files with the extension .e00 can be converted to ARC/INFO vector maps (coverages) and INFO files by running the import.aml that is included in the database. This will import the export files and assign standard names (see below). Be sure to uncompress the MF-2385_6a.e00.gz file with the gzip utility before running the import.aml. Run import.aml from the ARC prompt in the directory containing the export files:

ARC: &run import.aml - run import.aml

Note that the ARC coverages and separate INFO files will be given standard names:

MF-2385_3.e00 (Susceptibility Database) is named susgrd_utm